NASA TECHNICAL MEMORANDUM

NASA TM X-73991

NASA TM X-73991

A REVIEW OF SEVERAL PROPULSION INTEGRATION FEATURES APPLICABLE TO SUPERSONIC-CRUISE FIGHTER AIRCRAFT

By Bobby L. Berrier and Staff,
Propulsion Integration Section

December 1976

NATIONAL AERONAUTICS AND SPACE ADMINISTRATION
LANGLEY RESEARCH CENTER, HAMPTON, VIRGINIA 23665

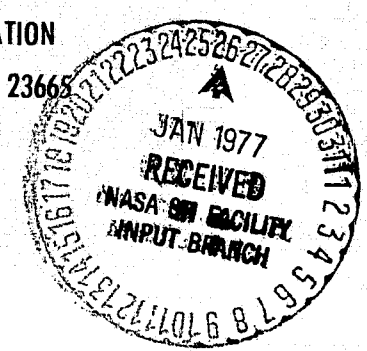

1. Report No.	2. Government Accession No.	3. Recipient's Catalog No.
NASA TM X-73991		

4. Title and Subtitle	5. Report Date
A Review of Several Propulsion Integration Features Applicable to Supersonic-Cruise Fighter Aircraft	December 1976
	6. Performing Organization Code
7. Author(s)	8. Performing Organization Report No.
Bobby L. Berrier and Staff, Propulsion Integration Section	
9. Performing Organization Name and Address	10. Work Unit No.
NASA Langley Research Center Hampton, VA 23665	505-04-11-01
	11. Contract or Grant No.
	13. Type of Report and Period Covered
12. Sponsoring Agency Name and Address	Technical Memorandum
National Aeronautics and Space Administration Washington, VA 20546	14. Sponsoring Agency Code

15. Supplementary Notes

Special technical information release, not planned for formal NASA publication.

16. Abstract

A brief review has been made of the propulsion integration features which may impact the design of a supersonic-cruise fighter-type aircraft. The data used for this study were obtained from several investigations conducted in the Langley 16-foot transonic and 4-by 4-foot supersonic presssure wind tunnels. Results of this study show: (1) that for conventional nozzle installations, contradictory design guidelines exist between subsonic and supersonic flight conditions; (2) that substantial drag penalties can be incurred by use of dry power nozzles during supersonic cruise; and (3) that a new and unique concept, the nonaxisymmetric nozzle, offers the potential for solving many of the current propulsion installation problems.

17. Key Words (Suggested by Author(s)) (STAR category underlined)	18. Distribution Statement
Supercruiser Propulsion Integration Nonaxisymmetric Nozzle Aerodynamics Vectoring	Unclassified Unlimited

19. Security Classif. (of this report)	20. Security Classif. (of this page)	21. No. of Pages	22. Price*
Unclassified	Unclassified	56	$4.50

*Available from (The National Technical Information Service, Springfield, Virginia 22161

SUMMARY

A review has been made of the propulsion integration features which may impact the design of a supersonic-cruise fighter-type aircraft. The data used for this study were obtained from several investigations conducted in the Langley 16-foot transonic and 4-by 4-foot supersonic pressure wind tunnels. Results of this study show: (1) for conventional nozzle installations, contradictory design guidelines exist between subsonic and supersonic flight conditions; (2) substantial drag penalties can be incurred by use of dry power nozzles during supersonic cruise; and (3) a new and unique concept, the nonaxisymmetric nozzle, offers the potential for solving many of the current propulsion installation problems.

INTRODUCTION

Research on aircraft design relative to the installation of the propulsive exhaust system into the airframe has received increasing attention over the past ten years. Summaries of some of this effort are contained in references 1 through 4. In reference 1, Nichols indicated that from the viewpoint of performance, exhaust-nozzle/airframe integration is the most critical design feature of an aircraft. An indication of the relative importance of this area is illustrated in figure 1. This figure presents a comparison of total airplane drag with aft-end (shaded region) drag for an "ideal" research model and a current aircraft development model. The afterbodies of these models comprised about one-third of the model length but produced 40 to 50 percent of the total configuration drag. The sum of the friction drag and the jet interference drag accounts for 40 to

50 percent of the drag on the afterbodies. The remainder is due to adverse interferences in the afterbody region and the pressure drag on the afterbody.

Most current operational military aircraft have been designed for efficient subsonic cruise and subsonic/transonic maneuverability; supersonic performance has been considered a "fallout" or off-design condition. As a result, past and current propulsion integration studies have emphasized the subsonic/transonic speed regime with little data being obtained at supersonic conditions. However, after analysis of the air operations during recent conflicts, much discussion has taken place in the United States concerning aircraft vulnerability over enemy territory; one method proposed to reduce aircraft vulnerability is to provide efficient supersonic cruise capability to future combat aircraft. The design guidelines for military supersonic-cruise fighter-type aircraft (so called "supercruiser") would be substantially different from those of current combat aircraft which have "fallout" or off-design supersonic performance and even from those of SST-type aircraft which have "fallout" or off-design subsonic performance. Indeed, the "supercruiser" mission may include both subsonic and supersonic cruise segments. In this case, neither the subsonic or supersonic speed regimes can be considered as an off-design condition. Since many design guidelines tend to be contradictory for the subsonic and supersonic speed regimes, this greatly aggravates the exhaust-nozzle/airframe integration problem which has already been shown to be substantial. (See fig. 1.) Supersonic cruise with dry power (nonafterburning) has been suggested as one method of improving supersonic cruise efficiency. Since

current fighter aircraft require afterburning power to fly at supersonic speeds, data on closed-down, dry power nozzles at Mach numbers above 1.3 are almost totally nonexistent. Although this feature could reduce specific fuel consumption and also IR signature, with current engines it could also accentuate nozzle/airframe integration problems at supersonic speeds because of increased boattail angle and closure area.

Material for this paper has been taken primarily from investigations conducted in the Langley 16-foot transonic tunnel and the Langley 4- by 4-foot supersonic pressure tunnel. The objectives of this paper are: (1) to provide a brief summary of some of the design features affecting nozzle/airframe integration with particular emphasis on differences between subsonic and supersonic design guidelines; (2) to provide an indication of the magnitude of nozzle/airframe integration problems associated with dry-power supersonic-cruise; and (3) to summarize the results of several investigations on a new and unique propulsion installation concept which has the potential of greatly reducing the nozzle/airframe integration problems associated with "supercruiser" subsonic and supersonic requirements.

It should be emphasized that many of the experimental results presented herein were obtained on relatively simple and clean afterbody configurations to indicate performance trends due to parametric variations. Effects of real aft-end complications can result in large reductions in performance compared with those of isolated aft-end models.

SYMBOLS

A	normal cross-sectional area, meters^2
A_e	nozzle exit area, meters^2
A_{max}	maximum afterbody cross-sectional area, meters^2
A_{ref}	reference wing area, meters^2
A_t	nozzle throat area, meters^2
C_D	airplane drag coefficient, $\frac{D}{q_\infty A_{ref}}$
$C_{D,a}$	afterbody (excluding nozzles) drag coefficient, $\frac{D_a}{q_\infty A_{max}}$
$C_{D,aft\text{-}end}$	aft-end (afterbody, nozzles and tails when present) drag coefficient, $\frac{D_{aft\text{-}end}}{q_\infty A_{max}}$
$C_{D,int}$	aft-end interference drag coefficient, $\frac{D_{int}}{q_\infty A_{max}}$
$C_{D,tails}$	tail drag coefficient, $\frac{D_{tails}}{q_\infty A_{max}}$
$C_{L,aft\text{-}end}$	aft-end lift coefficient, $\frac{L_{aft\text{-}end}}{q_\infty A_{ref}}$
D	airplane drag, newtons
D_a	afterbody (excluding nozzles) drag, newtons
$D_{aft\text{-}end}$	aft-end (afterbody, nozzles, tails when present) drag, newtons
D_{int}	aft-end interference drag, newtons

D_n	nozzle drag, newtons
D_{tails}	tail drag, newtons
d_m	maximum nozzle diameter, meters
F_i	ideal isentropic nozzle thrust, newtons
$L_{aft-end}$	aft-end lift, newtons
ℓ	nozzle length, meters
M	free-stream Mach number
$p_{t,j}$	jet exhaust total pressure, newtons/meter^2
p_∞	free-stream static pressure, newtons/meter^2
q_∞	free-stream dynamic pressure, newtons/meter^2
S	distance between twin-engine nozzle center lines, meters
T	measured nozzle thrust, newtons
x	length from model nose, meters
β	nozzle boattail angle, degrees
β_a	afterbody boattail angle approaching nozzle, degrees
Δ	incremental value
σ	resultant wedge camber angle, degrees

Abbreviations:

A/B	afterburning
C-D	convergent-divergent

conv.	convergent
IR	infrared
N.A.	not available
PR	nozzle pressure ratio, $p_{t,j}/p_\infty$

DISCUSSION

Conventional Nozzle Installations

Assuming sufficient fuel volume is available in a configuration with adequate supersonic performance, supersonic cruise in and out of enemy territory can be achieved by configurations with conventional exhaust system installations using afterburner (A/B) power. Figure 2 presents sketches of several conceptual "supercruiser" configurations with conventional nozzle installations. These configurations represent both single and twin engine designs with varying degrees of engine lateral spacing and adjacent airframe structure (tails, booms, etc.). The following paragraphs will briefly summarize the effects of these and other design features on max A/B nozzle/aft-end drag with particular emphasis on differences between subsonic and supersonic trends.

Engine/nozzle lateral spacing.- The effect of buried engine/nozzle lateral spacing on afterbody drag is presented in figure 3 for Mach numbers of 0.90, 1.30 and 2.20. These data were obtained from references 5, 6 and 7 for convergent, convergent-divergent and cone-plug nozzles, respectively. Airplane drag counts, obtained by using a wing reference area equal to ten times the model maximum cross-sectional area (rule-of-thumb for twin engine fighters), is presented as a function of engine spacing ratio (distance

between nozzle centerlines divided by maximum nozzle diameter). In general, the trend with increasing engine spacing ratio is identical at all Mach numbers, that is, afterbody drag increases with increasing spacing ratio. However, as illustrated by the average sensitivity constants (increase in drag obtained by increasing engine spacing by one nozzle diameter), sensitivity of afterbody drag to this design parameter increases significantly with Mach number. The sensitivity of afterbody drag to engine lateral spacing is three times the sensitivity at M = 2.2 as obtained at M = 0.9.

Twin-engine interfairing.- Figures 4 and 5 present the effect of twin-engine interfairing design on afterbody drag. Data on figure 4 were obtained from references 5, 7 and 8 and data on figure 5 were obtained from reference 9. A comparison of completely closed engine interfairings (no base) with ones having less closure area but terminating with a base is shown in figure 4. At subsonic speeds, the interfairings which are completely closed (no base) produced the lowest afterbody drag; at transonic speeds, mixed results were obtained; at supersonic speeds, the interfairings with less closure area and terminating with a base produced the lowest drag. The contradictory trends at subsonic and supersonic speeds are probably caused by the variation in jet interference effects as jet total-pressure ratio is increased with increasing Mach number to correspond to typical engine operating conditions. At subsonic speeds, the nozzle tends to be overexpanded and would thus aspirate any base region in close proximity to the jet exit and increase afterbody drag; at supersonic speeds, the nozzle tends to be underexpanded and would thus

pressurize any base region in close proximity to the jet exit and reduce afterbody drag.

Similar results to those shown on figure 4 are shown on figure 5 for the effect of interfairing length. At subsonic and transonic speeds, an interfairing which ends ahead of the nozzle exits produces the lowest afterbody drag; at supersonic speeds, an interfairing which extends downstream of the nozzle exits produces the lowest drag. The reason for this reverse in trends is probably caused by a variation in jet interference similar to that discussed for the data of figure 4.

The contradictory subsonic and supersonic design trends illustrated by figures 4 and 5 are indicative of the problems faced by the aircraft designer who must design aircraft to operate efficiently at both subsonic and supersonic flight conditions.

Outboard fairings (booms).- The effect on afterbody drag of outboard fairings or booms, located adjacent to and downstream of the nozzles, is shown in figure 6. Afterbody drag, booms on and off, is presented as a function of Mach number for typical engine operating jet total-pressure ratios at each Mach number. Afterbody drag was generally increased by addition of outboard fairings or booms. However, the sensitivity of afterbody drag to the addition of outboard booms decreases with increasing Mach number up to M = 2.0 where afterbody drag with booms on is approximately equal to afterbody drag with booms off. The decreased sensitivity of afterbody drag to the addition of outboard booms at supersonic Mach numbers is probably a result of beneficial jet effects at the higher engine operating jet total-pressure ratios associated with supersonic flight. These

results are similar to those discussed previously for the inboard engine interfairing (figs. 4 and 5). Comparison of the data shown on figure 6 with those shown on figure 5 shows that a drag crossover occurs for the outboard boom at $M \approx 2.0$ while for the inboard or engine interfairing, the drag crossover point occurs at $M \approx 1.3$. The lower Mach number at which an extended inboard engine interfairing becomes beneficial (fig. 5) when compared to an extended outboard boom (fig. 6), can be attributed to favorable jet effects on both sides of the extended inboard engine interfairing, while beneficial jet effects are limited to one side of the extended outboard boom.

The results presented in figures 4 through 6 are probably highly configuration dependent. Of more importance, since afterbody drag sensitivity to these design features depends to a great extent on jet interference effects, the results are highly dependent on the selected engine cycle. A "supercruiser" configuration with an engine cycle (operating PR) greatly different from that used for the present paper could result in significantly different drag sensitivities to these design features.

Approach boattail angle.- Another variable in the design of an aircraft afterbody is the boattail angle immediately upstream of the nozzle (approach angle). The effect of approach boattail angle on exhaust-nozzle performance is shown in figure 7. These data were obtained from reference 4. Approach boattail angles of 3°, 6° and 9° were tested with nozzles of the iris-convergent type. Exhaust-nozzle performance is defined as measured jet-thrust minus nozzle-external-drag, taken as a ratio of ideal

jet-thrust. At M = 0.7, pressure recovery in the external stream exerts a thrust on the nozzle external surface. This favorable pressure recovery becomes more pronounced as the approach boattail angle is increased such that, for $\beta_a = 9^o$, nozzle performance exceeds unity. At transonic and supersonic speeds, however, the external flow exerts a pressure drag on the nozzle outer surface and degrades performance. This adverse effect at supersonic speeds also increases with increasing boattail angle. Again the aircraft designer is faced with contradictory design guidelines.

The overall effect of approach boattail angle on nozzle performance and afterbody drag is assessed as follows: For aircraft having primary missions at subsonic speeds, moderately large values of nozzle approach boattail angle may be used without adverse effects on overall performance. For best performance of a supersonic aircraft, the nozzle approach boattail angle should be kept to a small value.

Tail location.- For stability and control purposes, aircraft have generally been designed with tail surfaces in an aft location. For some aircraft, the tail is mounted on booms such that the trailing edge is downstream of the nozzle exit. Data from reference 10 ($M \leq 1.2$) indicate that tail location can have a significant effect on afterbody/nozzle drag. Figure 8 presents empennage interference drag coefficient increments (positive values are unfavorable) as a function of Mach number for several empennage arrangements. Empennage interference drag increments were obtained as follows:

$$\Delta C_{D,int} = (C_D)_{\text{tails on}} - (C_D)_{\text{tails off}} - C_{D,\text{tails}}$$

where $(C_D)_{\text{tails on}}$ is the experimentally measured value of afterbody/nozzle/tail drag, $(C_D)_{\text{tails off}}$ is the experimentally measured value of afterbody/nozzle drag, and $C_{D,\text{tails}}$ is a computed value of tail drag. Tail drag was composed of friction drag plus form drag at subsonic speeds and friction drag plus wave drag at supersonic speeds. These data show that empennage interference on aft-end drag is adverse for all empennage arrangements tested. Empennage interference is generally small for $M < 0.85$, but increases dramatically at transonic and supersonic speeds. For Mach numbers less than 1.0, empennage interference was significantly reduced by staggering the vertical and horizontal tail surfaces. At supersonic speeds, empennage interference remains nearly constant with the lowest empennage interference being obtained on the forward empennage arrangement although this arrangement was not significantly better than the staggered empennage arrangement. It should be noted that the most adverse empennage interference was obtained for the aft or conventional tail location for most test conditions.

Local area rule bumps.- Addition of tail surfaces to a smoothly contoured afterbody creates a nonoptimum variation in the aft-fuselage area distribution as indicated by the lower sketch on figure 9. In an attempt to fill in and smooth the aft-fuselage normal-area-distribution and thereby hopefully reduce afterbody/nozzle drag, the investigation reported in reference 10 added area rule "contour" bumps around the tail surfaces on the afterbody. These "contour" bumps were designed for a $M = 1$ area cut and the resulting "smooth" normal-area-distribution is illustrated by the upper sketch on figure 9. The variation of afterbody/

nozzle drag, bumps on and bumps off, with Mach number is shown in figure 9 for a staggered empennage arrangement. For this configuration, addition of "contour" bumps was detrimental at all Mach numbers. However, this design feature appears to be configuration dependent since results from reference 10 show drag reductions attributable to the "contour" bumps for an aft empennage arrangement (dry power nozzle) in the transonic speed regime ($0.85 < M < 1.2$). At subsonic speeds, "contour" bumps were detrimental for all configurations investigated.

Local afterbody contouring.- An alternate approach to smoothing the aft-fuselage normal-area distribution is also reported in reference 10. Rather than adding area to fill in the area distribution, the afterbody was locally contoured to remove lumps created by the addition of tail surfaces. Sketches of area distributions illustrating this procedure, which was tried on the staggered empennage arrangement only, are presented as part of figure 10. The area distribution shown in figure 10 for the fully contoured afterbody is identical to the area distribution for the basic afterbody with tails off except for a range of x/ℓ from 0.85 to 0.95 where a small lump occurs. This lump occurs because a restriction was placed on the amount of afterbody contouring allowed (afterbody minimum diameter equal to nozzle maximum diameter), and also because the trailing edge of the horizontal tails extended aft of the nozzle connect station for this configuration. Figure 10 presents the variation of basic (uncontoured) and contoured afterbody/nozzle drag with Mach number. Data for a partially contoured afterbody (total tail cross-sectional area not removed from afterbody) are shown at a Mach number of 2.2 only. These

results show that afterbody contouring increased total aft-end drag at subsonic and high supersonic Mach numbers. However, drag reductions were obtained for Mach numbers between 1.2 and approximately 1.8, probably because the contoured afterbodies were designed for a M = 1 normal-area distribution. Afterbody contouring designed with higher Mach number area cuts could reduce aft-end drag at the higher supersonic Mach numbers but may cause greater afterbody/nozzle drag increases in the subsonic and transonic speed regimes.

Summary of design features.- The previous discussion briefly summarized the effects of some of the design features which might be found on a future "supercruiser" design. Examination of these results has shown that in almost every instance, contradictory design guidelines exist between subsonic and supersonic conditions (e.g. high subsonic drag sensitivity/low supersonic drag sensitivity, low subsonic drag sensitivity/high supersonic drag sensitivity, reversed trends, etc.). If one were designing either a subsonic or a supersonic point design aircraft, it would be a relatively easy task to select the proper design guidelines. However, as previously mentioned, the "supercruiser" design may be required to operate efficiently for long periods of time at both subsonic and supersonic flight conditions. Supersonic cruise with dry (nonafterburning) power has been suggested as one method of solving this apparent problem.

Dry Power/Supersonic Cruise Concept

Although many current military aircraft can operate at supersonic speeds by use of afterburning (A/B) power, their time at supersonic speeds is usually extremely limited because of the significant increase in specific

fuel consumption as engine power is increased from dry to afterburner operation. Assuming the proper engine cycle and aircraft aerodynamics can be determined, one unconventional technique suggested for efficient supersonic cruise is to use dry engine power only. Afterburning power would be provided for emergency use only. Since most current aircraft require afterburning power to fly at supersonic speeds, data on closed-down, dry power nozzles at supersonic speeds are almost totally nonexistent. The following paragraphs examine a small amount of data at Mach numbers up to 1.3 to give an indication of the possible problems one might encounter at supersonic cruise with dry power nozzles.

Dry power thrust-minus-drag.- Figure 11 presents the variation of aft-end thrust-minus-drag ratio with Mach number for four different nozzle concepts at both dry and max A/B power settings. These data were obtained from reference 11 and are presented at each Mach number for a typical engine operating jet total-pressure ratio. All nozzle types at both power settings exhibit similar performance at subsonic speeds with the dry power nozzles being somewhat inferior at the higher subsonic Mach numbers. However, at the low supersonic Mach numbers, the dry power nozzles exhibit a large thrust-minus-drag performance penalty when compared to the performance of their max A/B power counterparts. This penalty ranges from approximately 20 percent of the ideal nozzle thrust for the blow-in-door nozzle to 30 percent of the ideal nozzle thrust for the convergent-divergent nozzle. These performance losses are extremely large and, in fact, overshadow any effects discussed previously for other propulsion integration design features. Since the dry-power nozzles were designed

to operate efficiently at subsonic cruise, part of the performance loss at M = 1.2 and 1.3 can be attributed to internal performance losses associated with nonoptimum internal expansion ratios; however, a vast majority of the loss is due to increased drag on the dry power nozzle external surface. For example, at M = 1.3, PR = 4.9, the internal performance of a nozzle with an expansion ratio of 1.0 (convergent) would be approximately 0.972 compared with 0.98 to 0.99 for a nozzle with optimum expansion ratio. Thus only 2 percent of the 20- to 30-percent performance loss at M = 1.3 can be attributed to internal performance.

Interference on dry power nozzles.- The previous data, shown in figure 11, were obtained on a close-spaced, clean afterbody model. As illustrated in figure 2, "real" aircraft may have booms, tails, etc. in close proximity to the exhaust nozzle. As discussed previously for max A/B power configurations, these "real world" items can cause additional performance penalties due to adverse interference effects. Data from reference 4 are presented in figure 12 to illustrate the difference in interference effects on dry power and max A/B power nozzles. Figure 12 shows the variation with Mach number of the change in exhaust nozzle performance caused by adding outboard booms to a basic twin-engine afterbody, the increment being expressed as a fraction of ideal nozzle thrust. With max A/B nozzles installed, adverse boom interference was relatively small. At subsonic speeds, nozzle performance was reduced by approximately 1 percent of ideal gross thrust; at supersonic speeds, boom interference on the max A/B nozzle was negligible. However, examination of the dry-power nozzle data shows a much higher sensitivity of nozzle performance to boom

interference. At subsonic speeds, dry-power nozzle performance was reduced from 3.5 to 10 percent of ideal gross thrust; at supersonic speeds, adverse boom interference reduced performance by approximately 3 percent of ideal gross thrust. Data from reference 10 show a similar increased performance sensitivity of dry-power configurations to adverse tail interference effects. It should be noted that losses attributed to adverse interference effects (fig. 12) from booms, tails, etc., would be additive to the performance loss associated with basic configuration drag (fig. 11) caused by increased afterbody slopes and closure area.

Summary of dry-power/supersonic cruise concept.- Although the dry-power/supersonic cruise concept offers the potential of reduced specific fuel consumption and also IR signature, data on dry-power nozzle configurations at low supersonic speeds indicate that substantial performance penalties can be incurred. Very large penalties appear to be associated with the increased aft-end slopes and closure area of dry-power nozzle configurations (fig. 11) and an increased sensitivity to airframe/nozzle interference effects (fig. 12). Thus, it appears that inclusion of this feature on future aircraft designs may accentuate the substantial nozzle/airframe integration problems already discussed for "supercruiser" type configurations.

It should be noted that these conclusions are based on a data bank which almost totally excludes data above M = 1.3 and on current engines which have high ratios of maximum diameter to exit diameter (thus necessitating high closure slopes and areas). However, it is believed that the dry-power nozzle data presented for M = 1.2 and 1.3 do give an

indication of the problems which can be encountered.

Unconventional Nozzle Installations

The problems posed to the "supercruiser" designer by the contradictory subsonic and supersonic design guidelines, and the apparent high drag sensitivity of dry-power nozzles at supersonic speeds, may indicate the need for unconventional concepts. A "supercruiser" mission and configuration are yet to be defined; however a discussion of the most "talked about" qualities may be helpful in defining the exhaust system requirements. "Supercruiser" is:

- Low Vulnerability/High Survivability

  Supersonic cruise.- The "supercruiser" concept denotes supersonic cruise in and out of enemy territory. This requirement probably dictates a supersonic design.

  Subsonic self-defense capability (maneuverability).- Assuming a supersonic design and the contradictory design guidelines at subsonic and supersonic speeds previously discussed, this requirement will be difficult to meet. Thrust vectoring, thrust induced lift, and thrust reversing have been suggested as possible solutions to this problem.

  Low IR and RCS signatures.- This requirement would probably dictate a highly blended configuration with plug-type nozzles to hide hot engine parts.

  Low failure rate.- This requirement would indicate a simple exhaust system design and also possibly dictate a twin-engine configuration for one-engine-out/return-home capability.

- Efficient/Combat Effective

  Dry-power/supersonic cruise.- Supersonic Cruise with dry-power could significantly decrease specific fuel consumption and IR signature during supersonic flight.

  Low propulsion installation drag.- As discussed in a previous section, this requirement may be incompatible with dry-power/supersonic cruise for conventional installations. This problem may be insurmountable without innovative designs using unconventional concepts.

  Accurate weapons delivery.- This requirement and a desire for low vulnerability indicates a possible need for in-flight thrust modulation.

- Cost Effective

  Low cost/low maintenance.- This requirement would indicate a simple exhaust system design with minimum moving parts.

Recent DOD, NASA, and industry studies have shown that a new and unique propulsion installation concept, the nonaxisymmetric nozzle, offers the potential for obtaining most, if not all, of the above "supercruiser" exhaust system characteristics. Figure 13 presents a photograph comparing axisymmetric and nonaxisymmetric (2-D wedge) nozzle installations in a typical twin-engine, fighter-type configuration. Potential payoffs for this unique concept were identified in a recent U.S. Air Force funded study, reference 12. Several of the major payoffs identified are:

- Simple installation of thrust vectoring and reversing features with little penalty in weight and complexity.
- Integration benefits for up to 7 percent lower cruise drag.
- Improved subsonic maneuvering performance with thrust vectoring/thrust induced lift.
- Thrust reversal/modulation provides rapid in-flight deceleration and a reduction in landing ground roll.
- Centerbody nonaxisymmetric nozzles provide up to 90 percent reduction in IR signature with 45 percent reduction in IR lock-on range.
- Simplicity of nonaxisymmetric nozzles results in 84 percent fewer major components and 33 percent lower production cost.

This nonaxisymmetric nozzle study (ref. 12) also identified two major problem areas which must receive further study. These two problem areas are:

- Structures - the inherently poor structural efficiency of rectangular nozzles may preclude any overall structural weight advantage.
- Cooling - cooling losses associated with the increased wetted area of nonaxisymmetric nozzle designs may be somewhat larger than cooling losses of conventional designs.

Sketches of several conceptual "supercruiser" configurations with nonaxisymmetric nozzle installations are presented in figure 14. These configurations, similar to the conventional nozzle installations presented in figure 2, represent both single and twin engine designs with varying degrees of engine lateral spacing and adjacent airframe structure. However, unlike conventional nozzle installations, the nonaxisymmetric nozzle offers the additional flexibility of nozzle aspect ratio (for highly blended configurations), thrust vectoring (deflected wedge or upper-surface blowing), and thrust reversing. The following paragraphs will briefly summarize the results obtained from several wind-tunnel studies on a nonaxisymmetric 2-D wedge nozzle. These studies were conducted in the Langley 16-foot transonic tunnel and data are presented in references 13 through 15.

Single-engine performance.- A photograph of an isolated single-engine nonaxisymmetric nozzle model installed in the 16-foot transonic wind tunnel is shown in figure 15. This model was used to study the effects of internal expansion area ratio, nozzle boattail angle and wedge length on 2-D wedge nozzle performance.

Isolated nozzle performance at typical engine operating pressure ratios for several axisymmetric and two-dimensional wedge nozzle concepts is presented in figure 16. Shown in figure 16 is the closure area ratio $(A_m-A_t)/A_m$ which represents the amount of afterbody projected area which would result either in a boattailed fairing, base, or expansion surface. In every case for these comparisons, the closure area is greater for the two-dimensional wedge nozzles and thus may favor the axisymmetric thrust-minus-drag performance. The data of figure 16 indicate that at the static takeoff condition, the performance of the two-dimensional wedge nozzles

is about 1-1/2 percent to 2-1/2 percent of ideal thrust lower than that of the convergent nozzles, but is about the same as the axisymmetric cone plug nozzle. At subsonic cruise and transonic acceleration conditions, the two-dimensional wedge nozzles were found to be competitive with axisymmetric nozzles. A summary of the results obtained during these single-engine tests is presented in figure 17. It was determined during these tests that eliminating the wedge sideplates had little effect on nozzle performance. This result is significant in that elimination of the sideplates reduces hot wetted area and thus reduces cooling requirements. However, attempting to minimize hot wetted area by reducing wedge length, either by truncation or with a larger wedge half angle, resulted in large performance penalties.

Twin-engine performance.- Photographs of a twin-engine nonaxisymmetric nozzle installed in the Langley 16-foot transonic tunnel are shown in figure 18. The effects of the two empennage arrangements shown were investigated. The nozzle/aftbody design was based on the single engine model geometry but at a smaller scale. The aftbody contours had a 10^{o} boattail at the cowl trailing edge. Because of the data available from the single-nozzle test from which the effect of internal expansion area ratio was obtained, only one nozzle simulating dry-power geometry, with $A_e/A_t = 1.30$, was tested. An afterburner power nozzle geometry was also tested that had an internal expansion area ratio of 1.40.

Figure 19 presents a comparison of the twin-engine installation penalties for axisymmetric and 2-D wedge nozzles. Data are shown at Mach numbers of 0.0 and 0.9 for single-engine (solid symbols) and twin-

engine (open symbols) 2-D wedge nozzle installations on the left side and axisymmetric installations on the right side of the figure. Aft end thrust-minus-drag ratio is presented as a function of jet total-pressure ratio. The performance levels of the single- and twin-engine 2-D wedge nozzle installations are essentially identical for both Mach numbers shown. This result indicates that the twin-engine installation penalty is negligible for the 2-D wedge nozzle installation. This is not the case for the conventional axisymmetric nozzle installation as shown on the right side of figure 19. The performance levels at M = 0 for the single- and twin-engine axisymmetric nozzle installations agree within the accuracy of the data. This result is expected since drag equals zero at M = 0. However, at M = 0.9, the performance level of the twin-engine axisymmetric nozzle installation is significantly lower than the single-engine installation. This result indicates a substantial penalty, caused by the boattailed gutter between the engines, for twin-engine conventional-nozzle installations.

Figure 20 presents dry power, twin axisymmetric/2-D wedge nozzle comparisons at several Mach numbers. All axisymmetric data shown on figure 20 were obtained from reference 11 which also indicated that this axisymmetric nozzle configuration produced the highest subsonic dry-power performance of those investigated. The data shown in figure 20 indicate that twin 2-D wedge nozzle performance at Mach numbers greater than 0.80 is higher than the highest performance reported in reference 11 for an axisymmetric, conventional nozzle installation. At Mach numbers below 0.8, the twin 2-D wedge nozzle installation is slightly inferior to the

axisymmetric nozzle installation. This low speed penalty, for the 2-D wedge nozzle installation, is associated with the 1.5- to 2.5-percent internal performance loss indicated at static conditions on figure 16. However, as Mach number increases, the propulsion integration benefits of the 2-D wedge nozzle (lower aft-end drag) start to compensate for the slightly inferior internal performance until a performance equality is reached at M = 0.80 with the conventional, axisymmetric nozzle installation. As Mach number is increased above 0.80, the 2-D wedge nozzle integration benefits continue to accumulate such that at M = 1.20, the dry power 2-D wedge nozzle installation is approximately 17 percent of F_i superior to the dry-power axisymmetric nozzle installation. This superior performance can be attributed to several causes. The improved integration qualities of the 2-D wedge nozzle is produced by a basic reduction in wetted area and the elimination of the boattailed gutter between the engines. Also, plug type nozzles require significantly less airplane aft-end closure than nonplug type nozzles. Discussion in previous sections has indicated that aft-end drag at transonic and supersonic speeds is particularly sensitive to aft-end closure slope and area. An indication of the importance of aft-end closure area can be obtained by a reexamination of figures 3 and 4. The reduced closure area of the axisymmetric plug nozzle installation produced the lowest afterbody drag for all test conditions shown. Finally, the iris-convergent nozzle expansion ratio (A_e/A_t) is not optimum for operation at M = 1.20. If the internal expansion ratio were increased to 1.30, to match engine operating PR, then the axisymmetric afterbody/nozzle performance would be increased by about 2 percent of the ideal thrust.

The data presented in figure 20 indicate that the dry-power 2-D wedge nozzle performance is clearly superior to the iris-convergent nozzle installation, particularly at M = 1.20. If supersonic, dry-power cruise is desired, the 2-D wedge nozzle is an attractive installation because of its high performance at transonic/supersonic speeds.

A comparison of the performance of a 2-D wedge, max A/B power nozzle installation with that of two different axisymmetric, max A/B power nozzle installations is shown in figure 21. The axisymmetric nozzles have the highest max A/B power performance reported in reference 11; these nozzles are of the convergent-divergent type. Similar results are shown for the max A/B power nozzle installations as discussed previously for the dry-power nozzle installations. One apparent difference is that the performance cross-over for max A/B power installations occurs at a lower Mach number (less than 0.8) than shown for dry-power installations.

Thrust vectoring characteristics.- Recent nonaxisymmetric nozzle studies have shown that thrust vectoring can significantly increase the maneuverability of a fighter airplane. As detailed in references 12 and 15, if lifting surfaces are properly integrated with the vectoring nozzle, jet-induced lift forces equal to or greater than the thrust lift vector can be achieved. Air-to-air combat advantages for vectored aircraft during one-on-one engagements were recently demonstrated in the NASA Langley differential maneuvering simulator.

To study the capability of the two-dimensional wedge nozzle to vector thrust by cambering the wedge, as illustrated by the left photograph on figure 22, thrust vectoring configurations were tested for wedge-

vectoring designs of 12^{o} and 24^{o}. The configuration shown in figure 22 is the 24^{o} cambered wedge. Thrust vectoring characteristics of the two cambered wedge designs without vertical tails at Mach 0.4 are presented in figure 23. Lift coefficient and the ratio of thrust-minus-drag to ideal thrust are presented as a function of nozzle pressure ratio. Lift coefficient was nondimensionalized by a typical wing reference area equal to 10 A_m. A component buildup of lift is given showing the tail lift, jet lift (thrust-lift vector) and the horizontal-tail, jet-induced lift variations with nozzle pressure ratio. As shown in figure 23, the jet induced-lift increment is equal to or greater than the thrust-lift vector increment. The 24^{o} vectored thrust configuration produced about twice the total lift increment as the 12^{o} wedge-vectored thrust configuration (ΔC_L of 0.35 compared to 0.20); however, the 12^{o} wedge-vectored thrust configuration was more efficient at producing jet-induced lift as compared to the jet lift increment. In addition, thrust-minus-drag losses for the 12^{o} wedge-vectored thrust configuration were only about 1 percent of ideal thrust compared to about 8 percent for the 24^{o} wedge-vectored thrust configuration at a typical flight nozzle pressure ratio. These losses are probably a result of exhaust flow separation from the upper surface of the wedge at the higher vector angles.

Thrust reversing characteristics.- The maneuvering benefits to be derived from in-flight thrust modulation or thrust reversing are discussed in reference 16. A thrust reversing or modulating system can easily be incorporated in the 2-D wedge nozzle by the installation of reverser panels in the manner shown by the right hand photograph of figure 22.

During the twin 2-D wedge nozzle investigation two reverser-panel positions were studied on the dry-power nozzle. One position represented a 50 percent deployment which symmetrically directed the exhaust 27° aft of the vertical plane passing through the nozzle exit. The other represented a 100-percent deployment which symmetrically directed the exhaust 45° forward of the same vertical plane. The configuration shown in figure 22 is the 100-percent deployment. The thrust reversing characteristics of the 50-percent and 100-percent deployed reverser geometry are shown in figure 24. The 50-percent deployed reverser geometry was intended to simulate a thrust spoiler position. The static thrust modulation or reverse thrust effectiveness is typical for current thrust reversers. At flight speeds, the reversing effectiveness sharply increases as a result of the base drag created by the reverser panels as they are deployed. Reverser base drag, determined from static pressure orifices located on the aft side of the reverser panels, contributes a substantial portion of the in-flight reverser effectiveness and is nearly constant with nozzle pressure ratio (fig. 24). The remaining contributors to in-flight reverse thrust are the reverser exhaust momentum (static) and an unaccounted-for component that is probably due to pressure drag acting on the wedge aft of the reverser panels. Because of the large base drag component, the in-flight reverse thrust effectiveness is excellent.

Summary of nonaxisymmetric nozzle concept.- A summary of the results from an investigation of a nonaxisymmetric nozzle concept (2-D wedge) in the NASA-Langley 16-foot transonic tunnel is presented in figure 25. This unique concept appears to be ideally suited to help the "supercruiser"

concept meet many of its desired goals. For example, the 2-D wedge nozzle concept offers the potential of providing low propulsion system installation drag through most of the Mach number range. Of particular significance is the vastly improved dry-power performance (T-D) of this concept over conventional dry-power nozzle installations at supersonic speeds. Propulsion system drag appears to be a critical technology for an aircraft design using dry-power to cruise at supersonic speeds. Thrust vectoring and reversing may help solve the subsonic self-defense problem of a supersonic aircraft design. Plug type nonaxisymmetric nozzle concepts offer reduced vulnerability by providing lower IR signatures and highly directional radar cross-sections to reduce missile lock-on range and provide "break-lock" capability. In-flight thrust modulation can provide better weapons delivery accuracy and lower vulnerability during air-to-ground operations. As discussed previously, nonaxisymmetric nozzles are simple in design and operation and thus reduce failure rate and production/maintenance cost.

Although the nonaxisymmetric nozzle concept offers potential for "supercruiser" type aircraft, much work remains to be done in the propulsion integration area. The nonaxisymmetric nozzle structural and cooling problems discussed previously must be adequately solved. In order to obtain maximum performance gains, vectored thrust propulsion systems must be properly integrated with the configuration lifting surfaces (in order to obtain thrust-induced lift). Results from the twin 2-D wedge nozzle test indicate a substantial loss of rudder and horizontal tail effectiveness during reverse thrust operation; reverse thrust propulsion systems must be

properly integrated with control surfaces to avoid this problem. If conventional nozzles are used on the "supercruiser" concept, the seemingly contradictory subsonic and supersonic guidelines must be resolved or at least adequate trades made. Also, if "supercruiser" is intended to cruise supersonically with conventional dry-power nozzles, the problem of excessive propulsion system drag must be attacked.

CONCLUSIONS

A brief review has been made of the propulsion integration features which may impact the design of a supersonic-cruise fighter aircraft. The data used for this study were obtained from several investigations conducted by the personnel of the Propulsion Integration Section at the Langley Research Center.

The results of this study indicate the following:

1. For conventional nozzle installations, contradictory design guidelines exist between subsonic and supersonic conditions for almost every design feature studied.
2. Supersonic cruise with dry power could result in reduced specific fuel consumption and infrared signature at supersonic speeds. However, available data in the M = 1.2 to 1.3 range indicate that substantial drag penalties will be incurred by conventional dry-power configurations at supersonic speeds. These penalties are associated with the increased aft-end slopes and closure area of these type configurations and also an increased sensitivity to airframe/nozzle interference effects.

3. A new and unique propulsion integration concept, the nonaxisymmetric nozzle with thrust vectoring and reversing features, has the potential to help solve many of the problems associated with propulsion system installation in supersonic-cruise fighter aircraft. This concept offers benefits in the areas of vulnerability, survivability, cruise and maneuvering performance, combat efficiency and cost. Problem areas of structural weight and cooling remain to be solved or minimized.

1. Nichols, Mark R.: Aerodynamics of Airframe-Engine Integration of Supersonic Aircraft. NASA TN D-3390, 1966.

2. Runckel, Jack F.: Jet-Exit and Airframe Interference Studies on Twin-Engine-Fuselage Aircraft Installations. NASA TM X-1274, 1966.

3. Corson, Blake W., Jr.; and Runckel, Jack F.: Exploratory Studies of Aircraft Afterbody and Exhaust-Nozzle Interaction. NASA TM X-1925, 1969.

4. Runckel, Jack F.: Interference Between Exhaust System and Afterbody of Twin-Engine Fuselage Configurations. NASA TN D-7525, 1974.

5. Maiden, Donald L.; and Runckel, Jack F.: Effect of Nozzle Lateral Spacing on Afterbody Drag and Performance of Twin-Jet Afterbody Models with Convergent Nozzles at Mach Numbers Up to 2.2. NASA TM X-2099, 1970.

6. Pendergraft, Odis C., Jr.; and Schmeer, James W.: Effect of Nozzle Lateral Spacing on Afterbody Drag and Performance of Twin-Jet Afterbody Models with Convergent-Divergent Nozzles at Mach Numbers Up to 2.2. NASA TM X-2601, 1972.

7. Berrier, Bobby L.: Effect of Nozzle Lateral Spacing on Afterbody Drag and Performance of Twin-Jet Afterbody Models with Cone Plug Nozzles at Mach Numbers Up to 2.2. NASA TM X-2632, 1972.

8. Lee, Edwin E., Jr.; and Runckel, Jack F.: Performance of Closely Spaced Twin-Jet Afterbodies with Different Inboard-Outboard Fairing and Nozzle Shapes. NASA TM X-2329, 1971.

9. Berrier, Bobby L.; and Wood, Frederick H., Jr.: Effect of Jet Velocity and Axial Location of Nozzle Exit on the Performance of a Twin-Jet Afterbody Model at Mach Numbers Up to 2.2. NASA TN D-5393, 1969.

10. Berrier, Bobby L.: Effect of Empennage Interference on Single-Engine Afterbody/Nozzle Drag. AIAA Paper No. 75-1296, 1975.

11. Mercer, Charles E.; and Berrier, Bobby L.: Effect of Afterbody Shape, Nozzle Type, and Engine Lateral Spacing on the Performance of a Twin-Jet Afterbody Model. NASA TM X-1855, 1969.

12. Hiley, P.E.; Wallace, H. W.; and Booz, D.E.: Study of Nonaxisymmetric Nozzles Installed in Advanced Fighter Aircraft. AIAA Paper No. 75-1316, 1975.

13. Maiden, Donald L.: Performance of an Isolated Two-Dimensional Variable-Geometry Wedge Nozzle with Translating Shroud and Collapsing Wedge at Speeds Up to Mach 2.01. NASA TN D-7906, 1975.

14. Maiden, Donald L.; and Petit, John E.: Investigation of Two-Dimensional Wedge Exhaust Nozzles for Advanced Aircraft. AIAA Paper No. 75-1317, 1975.

15. Capone, Francis J.: A Summary of Experimental Research on Propulsive-Lift Concepts in the Langley 16-Foot Transonic Tunnel. AIAA Paper No. 75-1315, 1975.

16. Linderman, D. C.; and Mount, J. S.: Development of an In-flight Thrust Reverser for Tactical/Attack Aircraft. AIAA Paper No. 70-699, 1970.

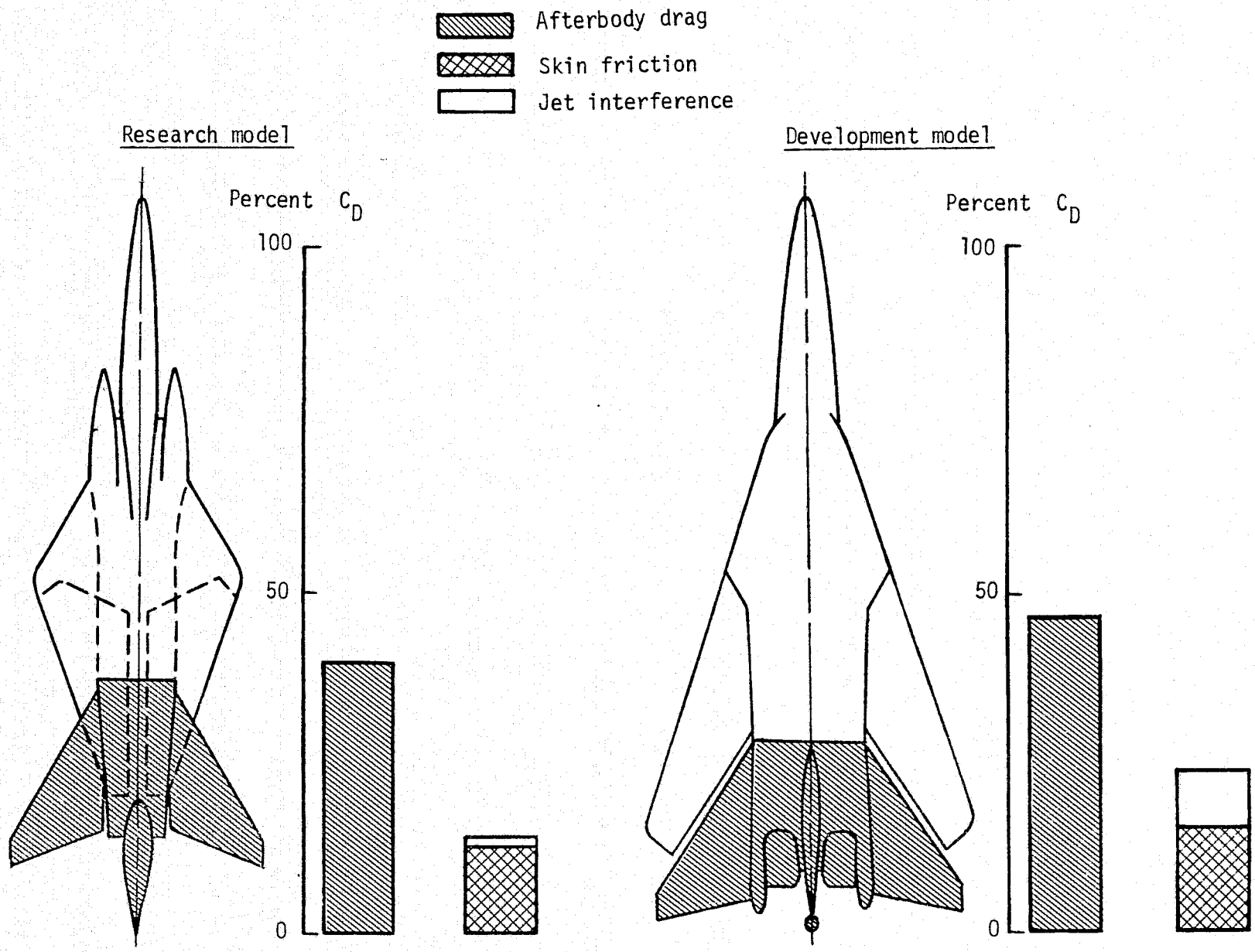

Figure 1.- Comparison of total and aft-end drag, M = 1.2 at sea level.

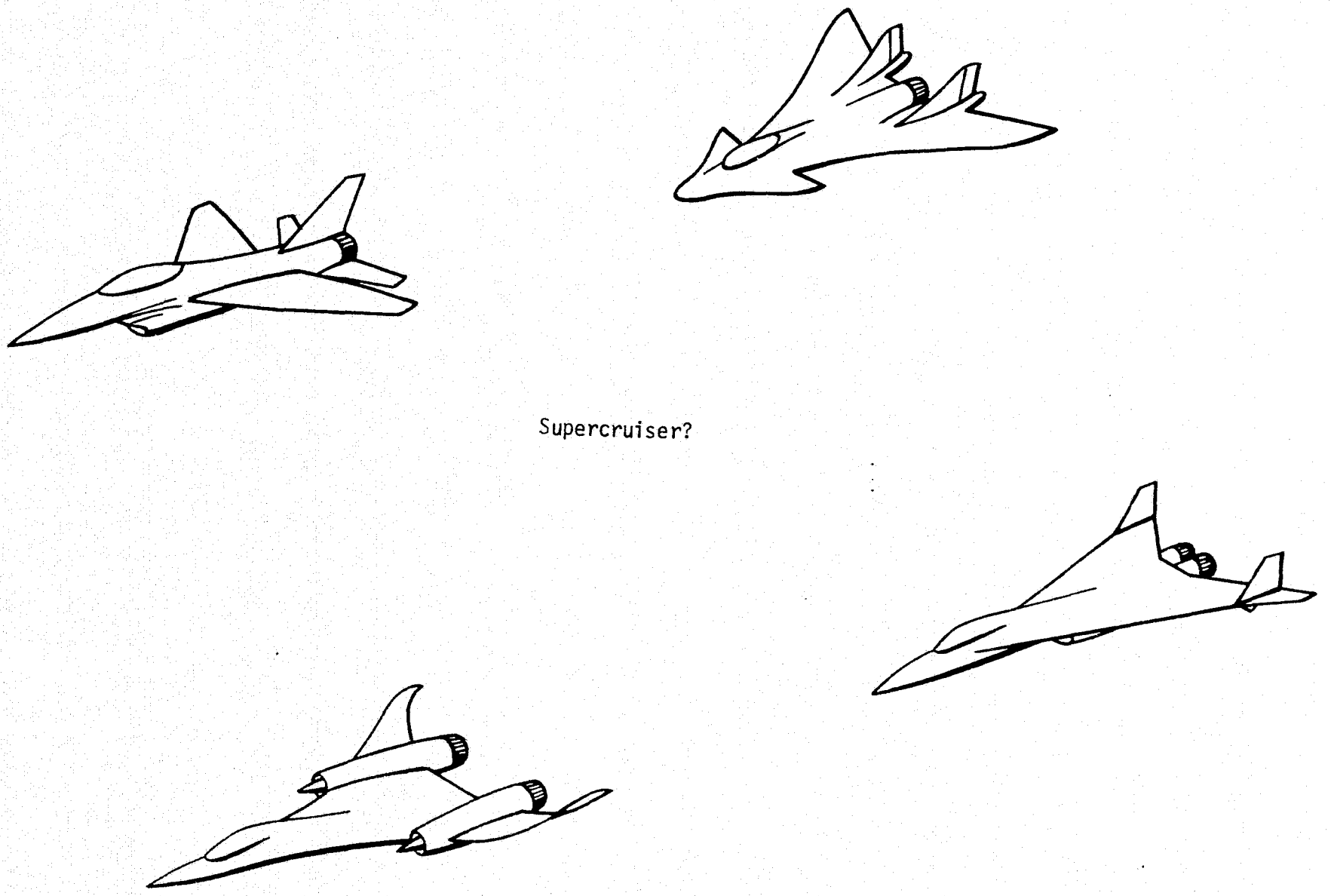

Figure 2.- Sketches of several conceptual "supercruiser" configurations with conventional nozzle installations.

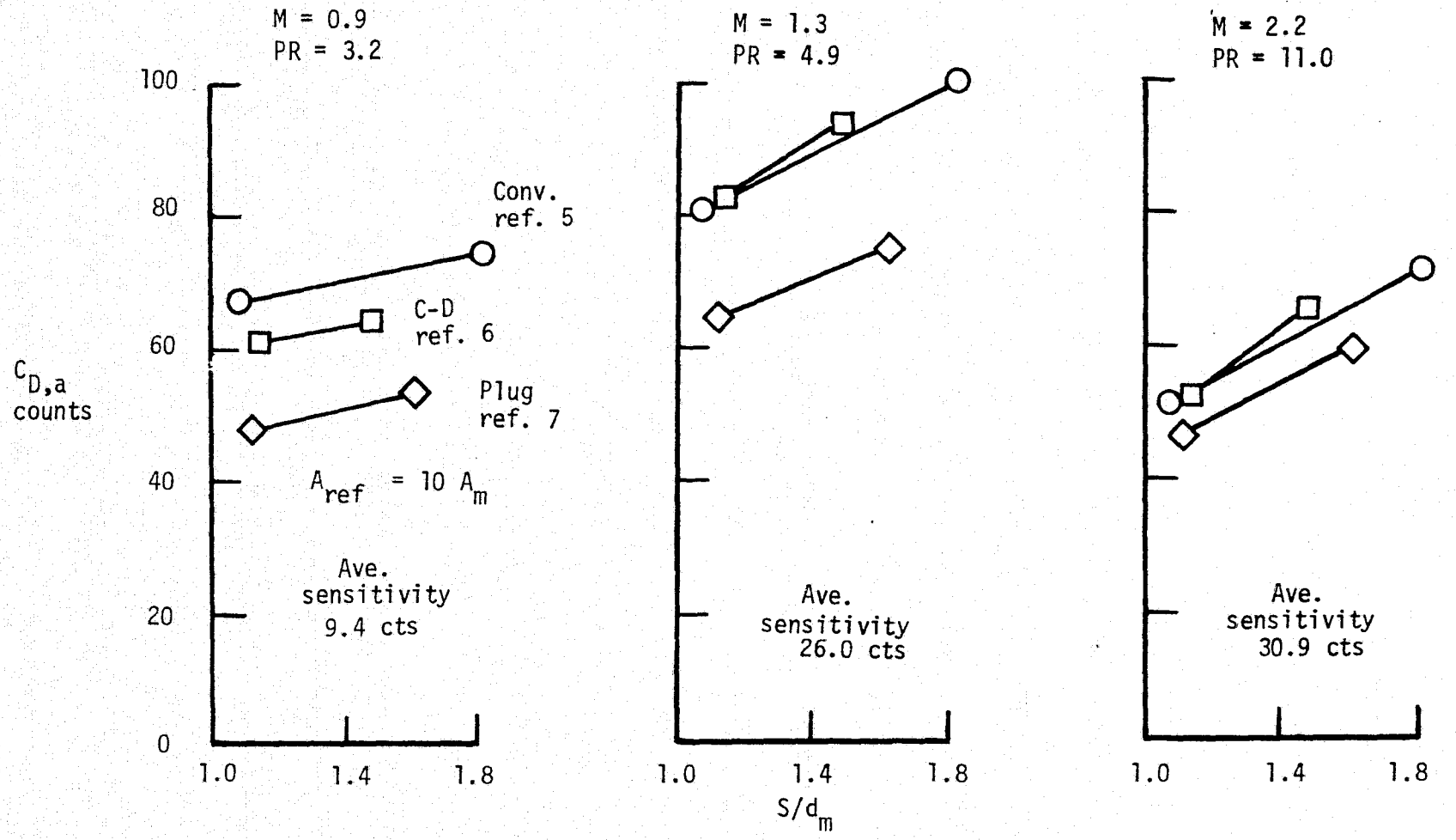

Figure 3.- Effect of lateral engine spacing on afterbody drag. Max A/B power nozzle.

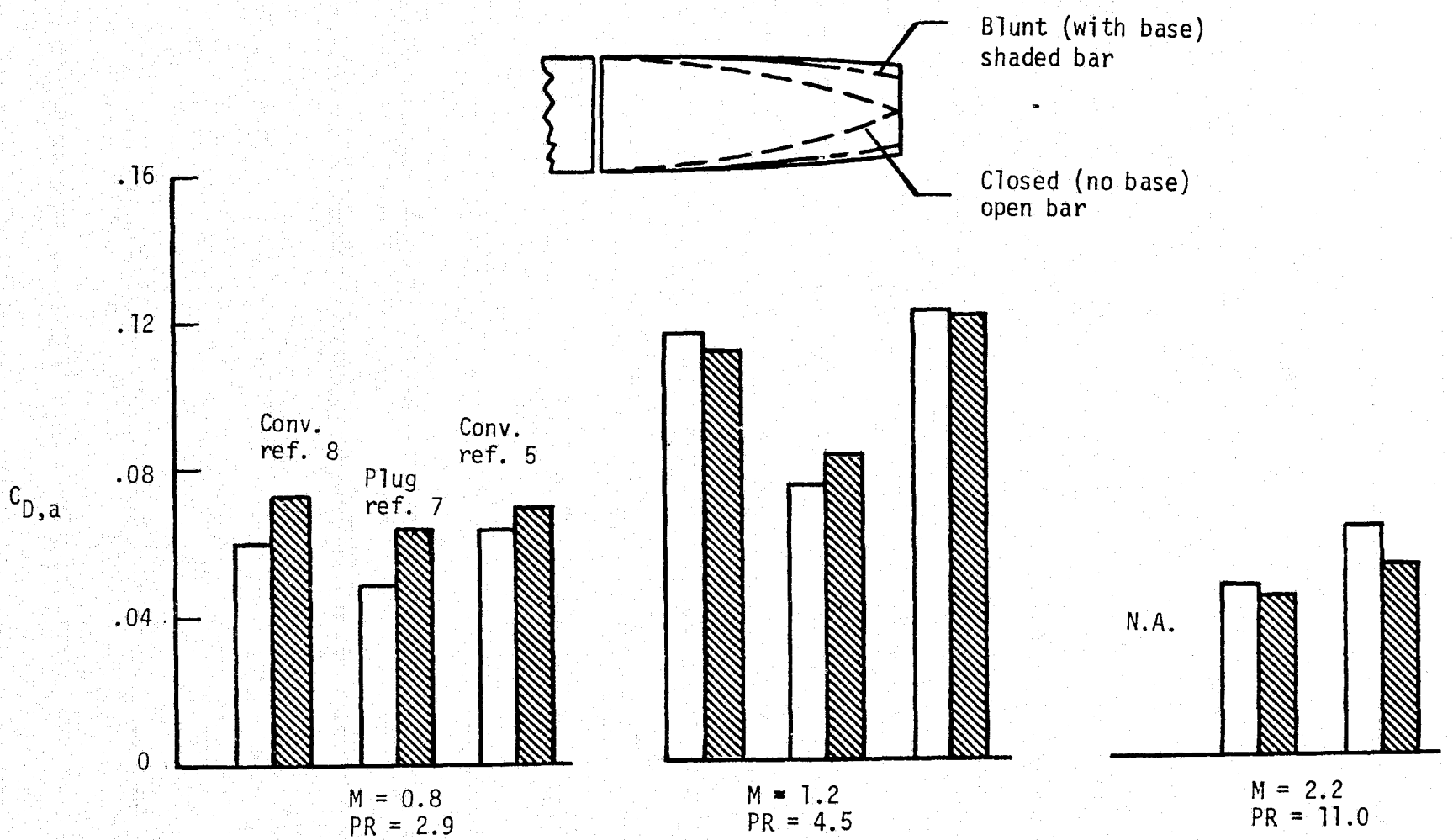

Figure 4.- Effect of engine interfairing design on afterbody drag. Max A/B power nozzles.

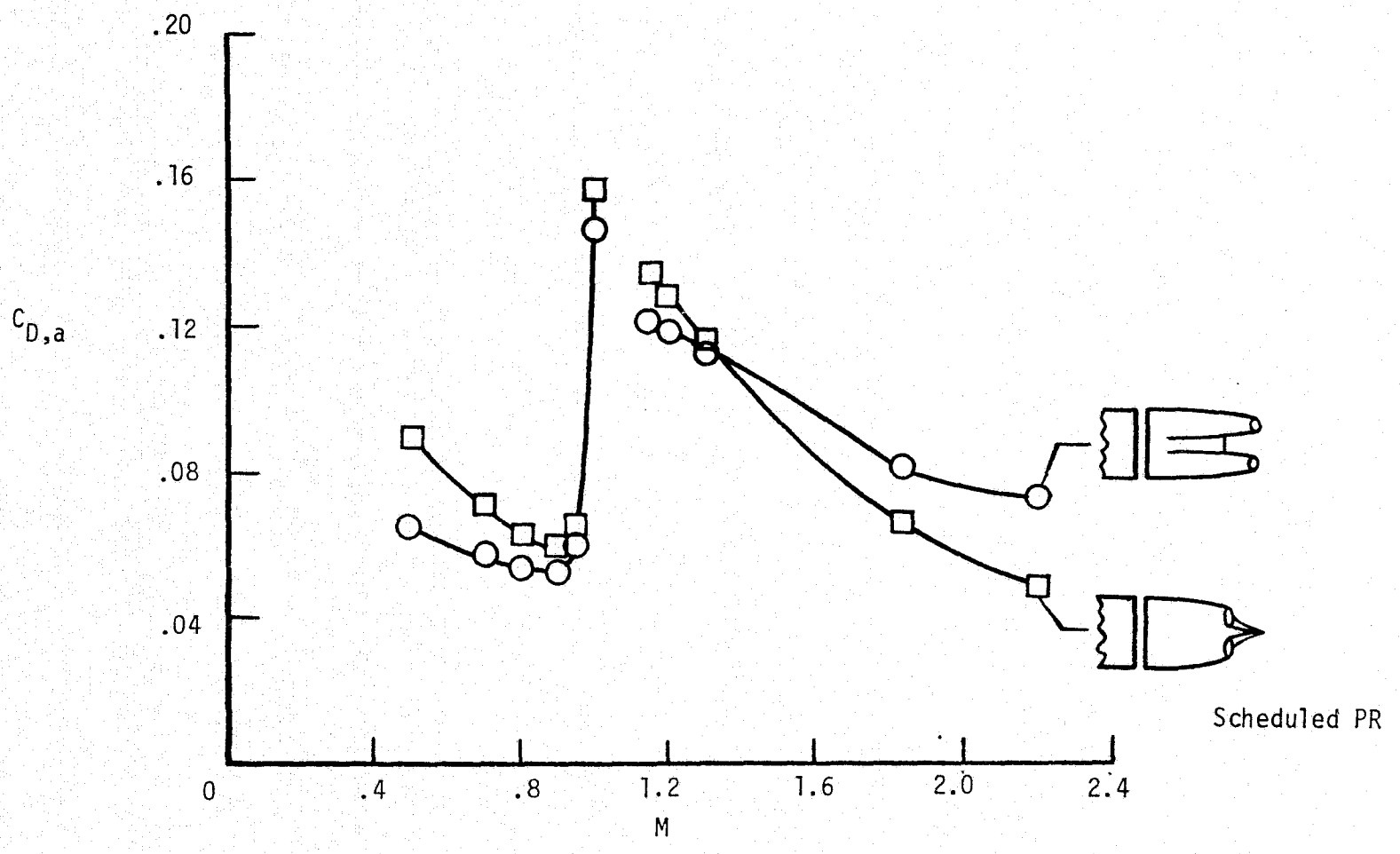

Figure 5.- Effect of engine interfairing design on afterbody drag.

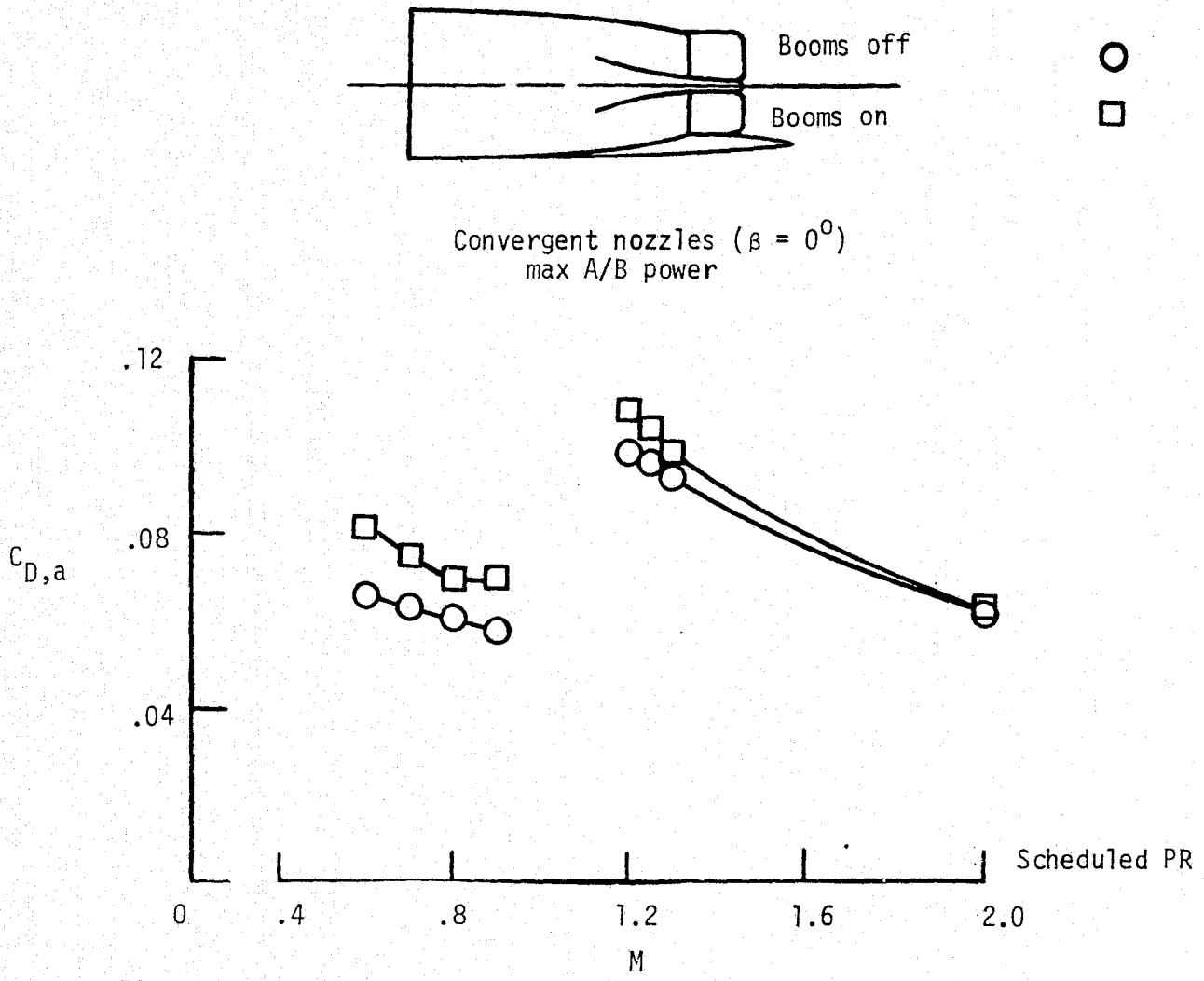

Figure 6.- Effect of outboard fairings or booms on afterbody drag.

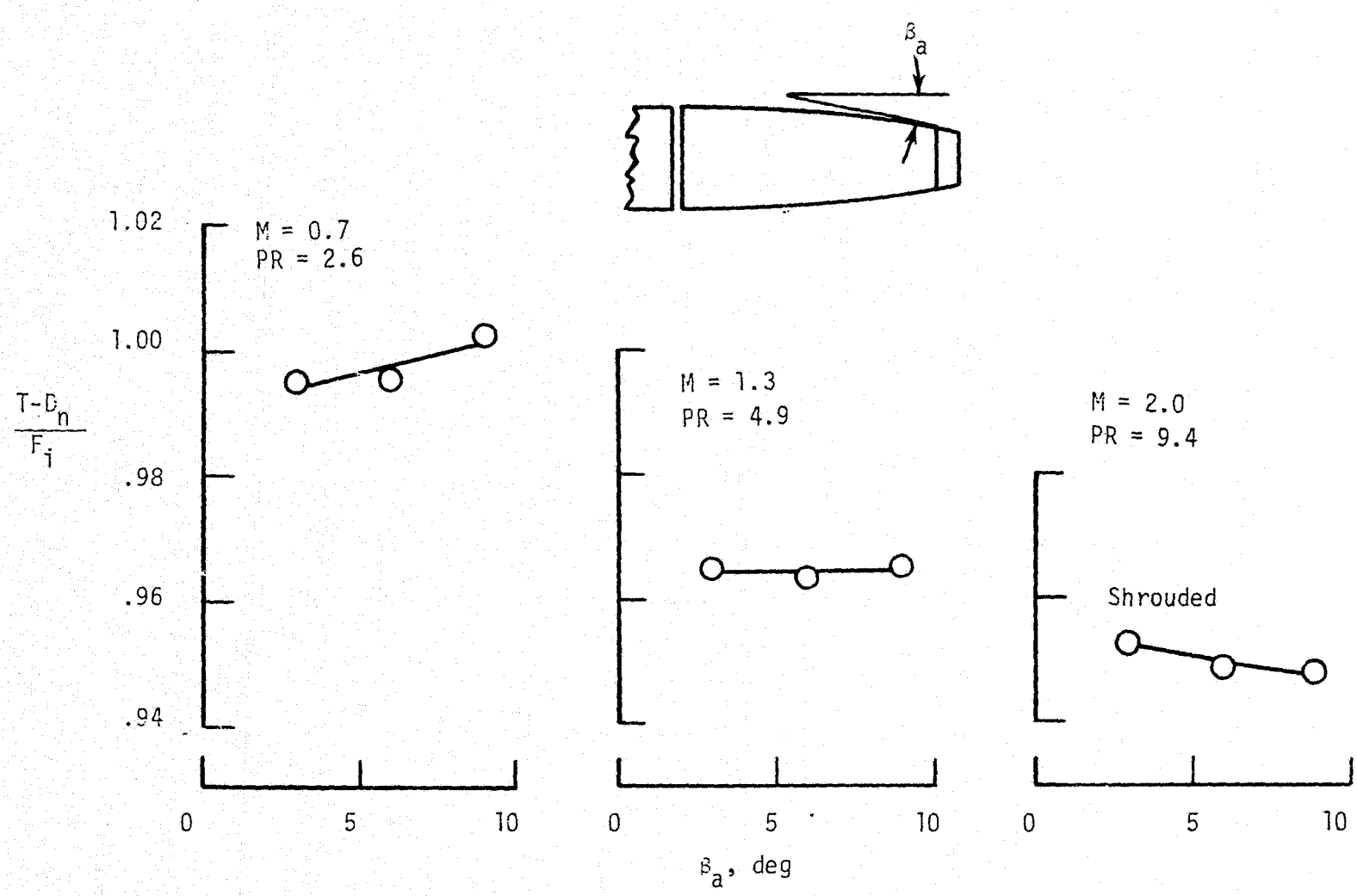

Figure 7.- Effect of approach boattail angle on nozzle performance. Max A/B power, reference 4.

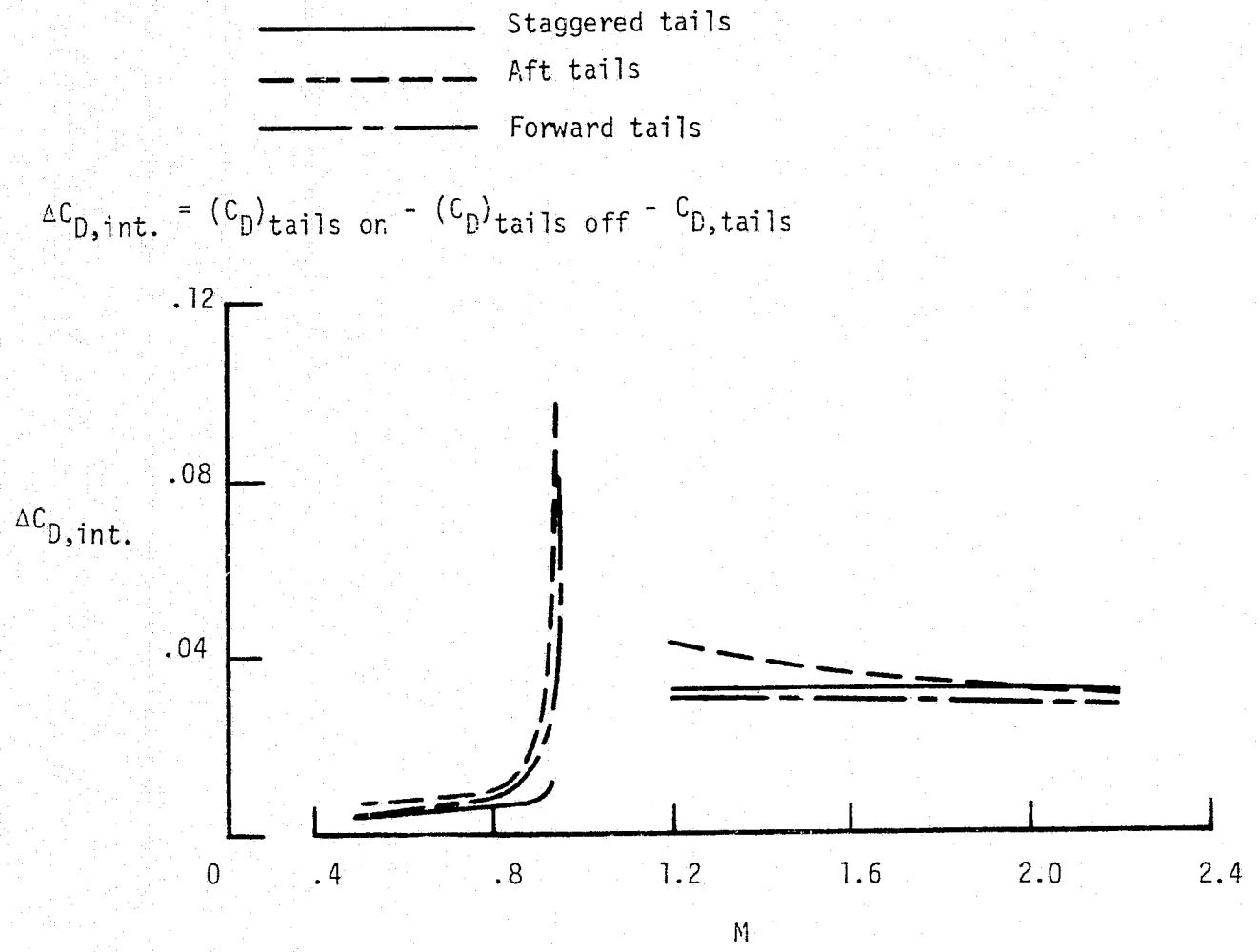

Figure 8.- Effect of tail location on afterbody/nozzle drag. Single-engine, max A/B power nozzle. Scheduled PR.

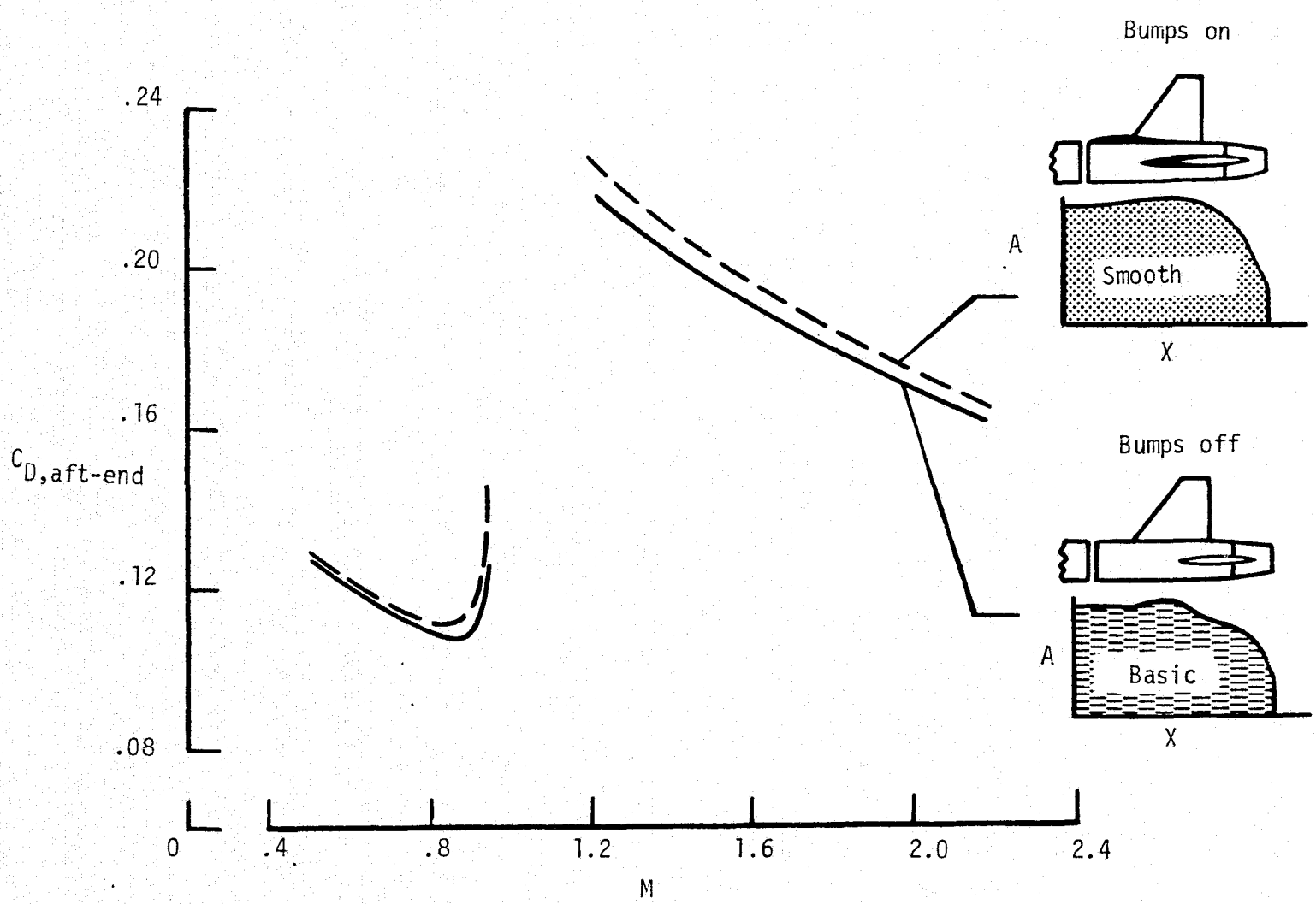

Figure 9.- Effect of local area rule bumps (M = 1.0) on afterbody/nozzle drag. Single engine-max A/B power nozzle. Staggered tails, scheduled PR.

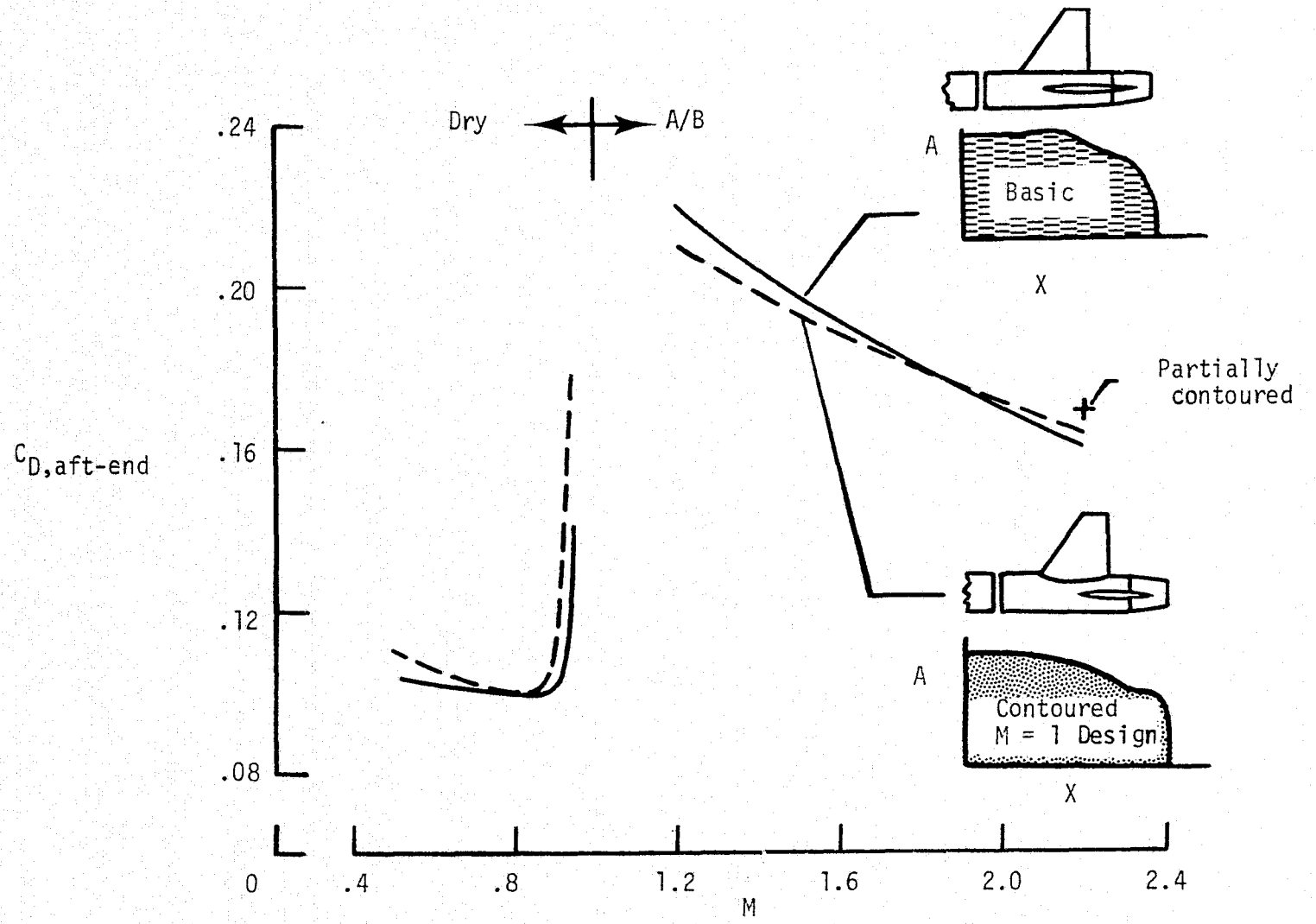

Figure 10.- Effect of local afterbody area ruling on afterbody/nozzle drag. Single engine. Staggered tails, scheduled PR.

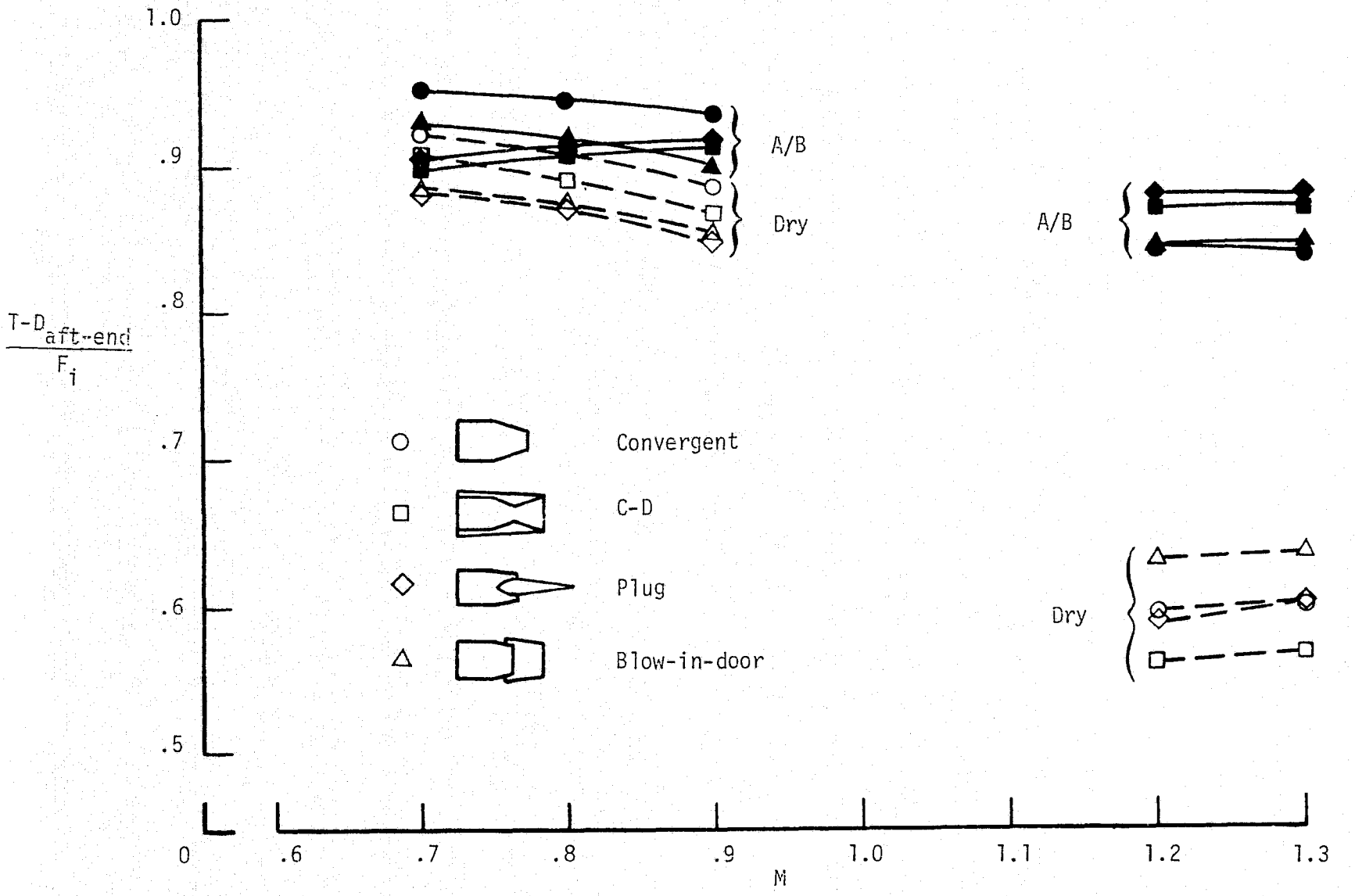

Figure 11.- Effect of nozzle power setting on aft-end thrust-minus-drag. Clean, close-spaced twin engine afterbody, scheduled PR.

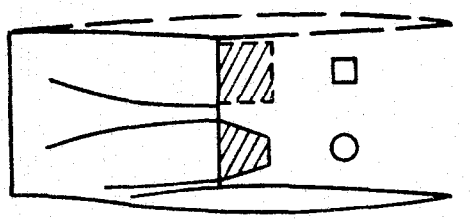

C-D Nozzles

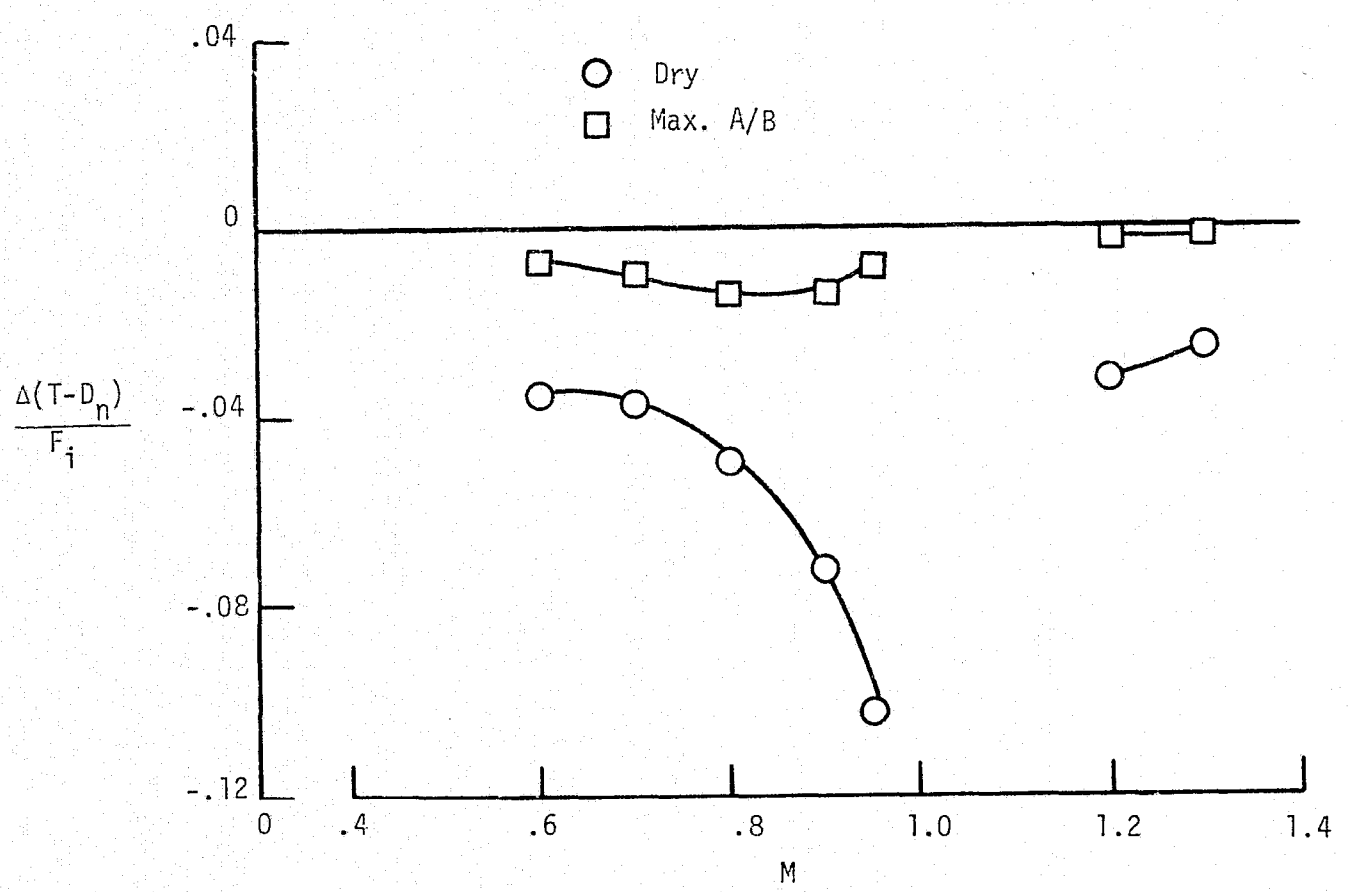

Figure 12.- Effect of power setting on boom interference. Scheduled PR.

Figure 13.- Photograph of typical axisymmetric and nonaxisymmetric nozzle installations in a twin-engine fighter-type configuration.

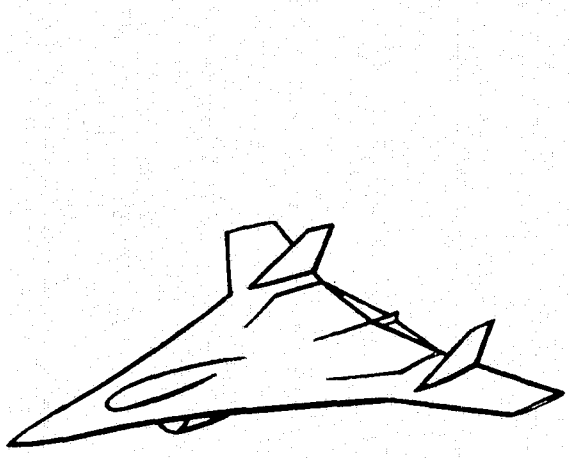

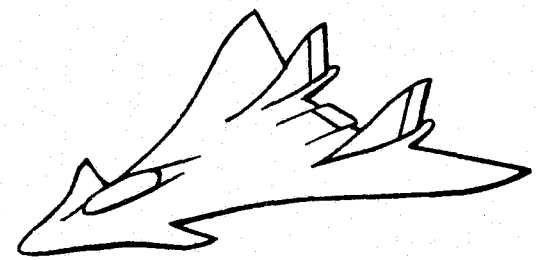

Supercruiser?

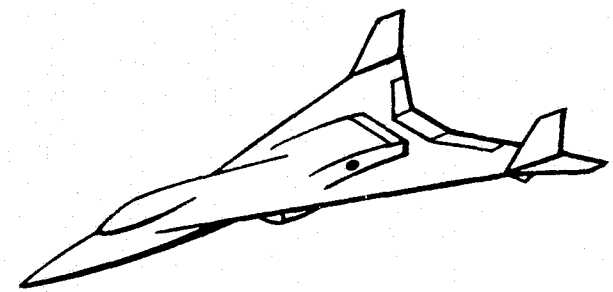

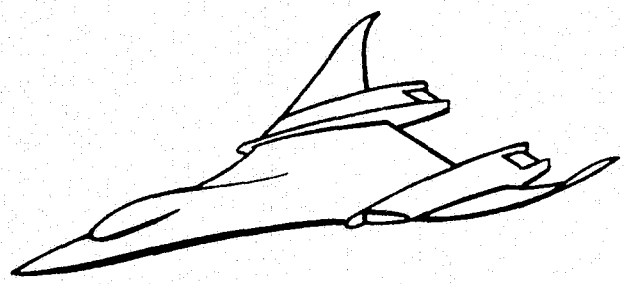

Figure 14. - Sketches of several conceptual "supercruiser" configurations with nonaxisymmetric nozzle installations.

Figure 15. - Single nozzle model installed in the Langley 16-foot transonic tunnel.

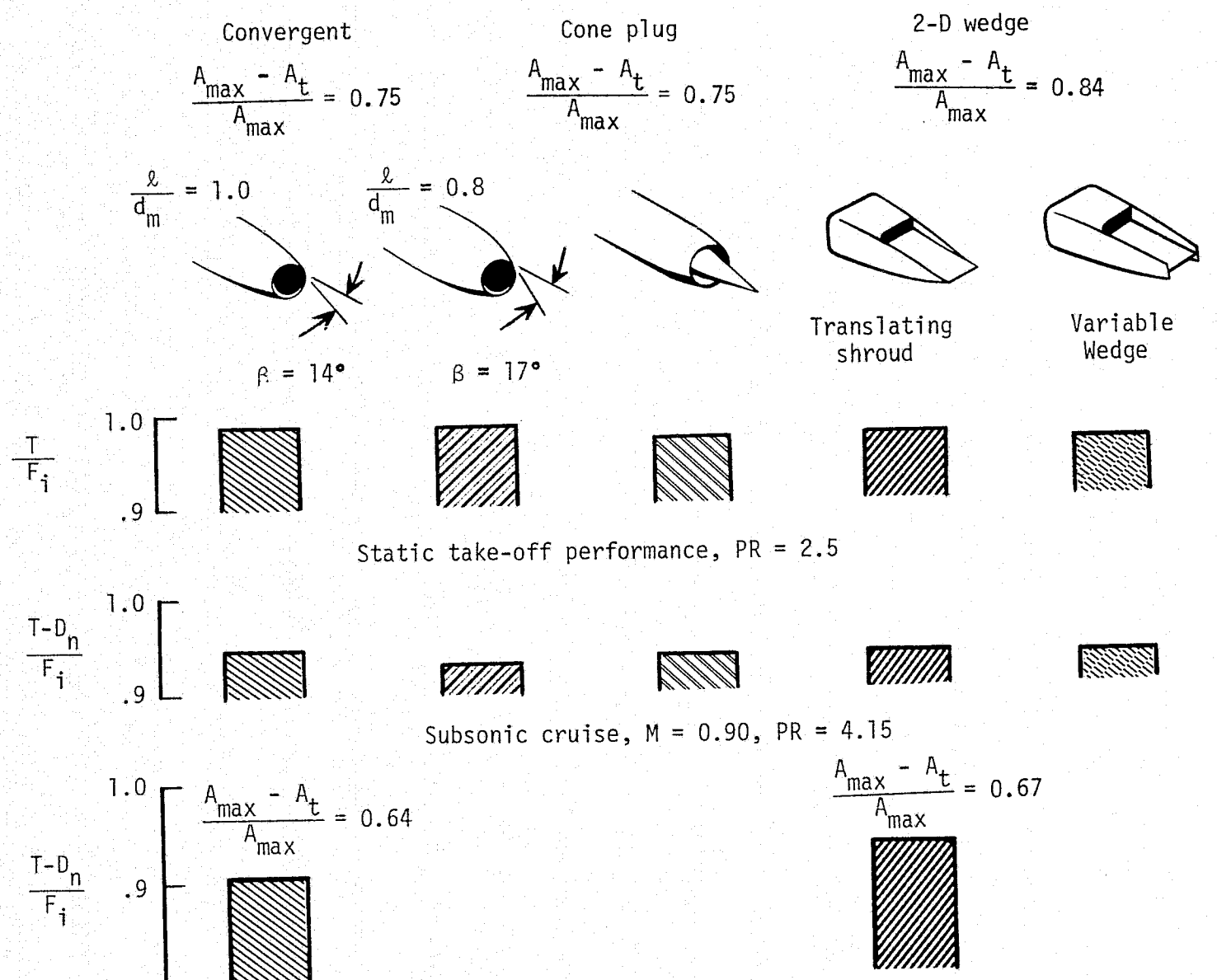

Figure 16. - Isolated nozzle performance.

Competitive with axisymmetric nozzles

Internal expansion critical $\left(A_e/A_t\right)$

Subsonic/transonic-variable 1.03 to 1.30
Transonic/supersonic-variable 1.30 to about 1.60

Cowl boattail angle $\geq$ wedge half-angle
supersonic penalty for steep boattail

No penalty to eliminate sideplate

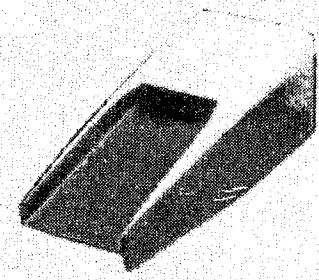

Shallow circular-arc boattail

Any wedge truncation detrimental

Wedge half-angle critical
-Shallow half-angle gave highest performance
-External wedge half-angle shallow for supersonic speeds

Figure 17. - Summary of single engine results.

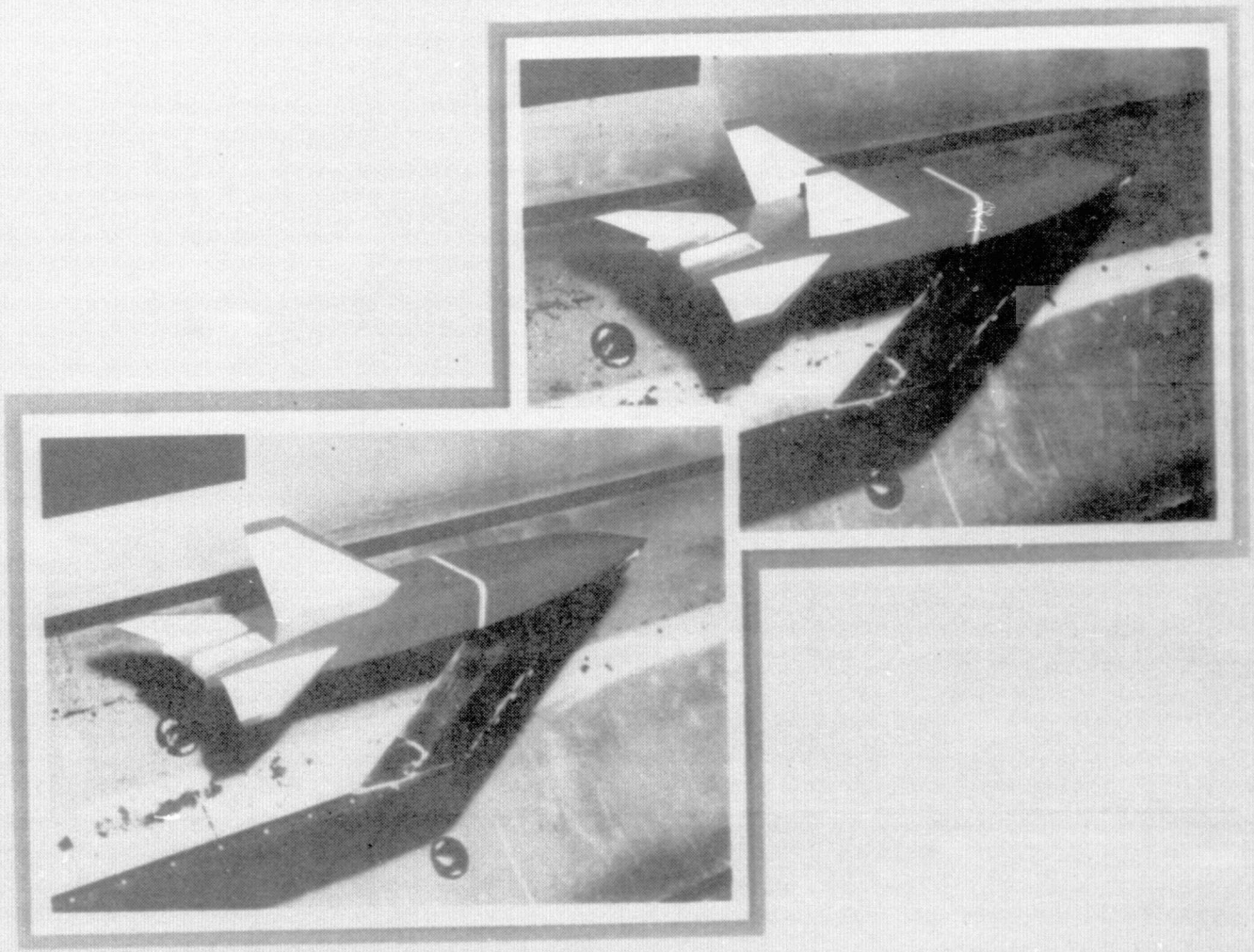

Figure 18. - Photographs of twin-engine model installed in the Langley 16-foot transonic tunnel.

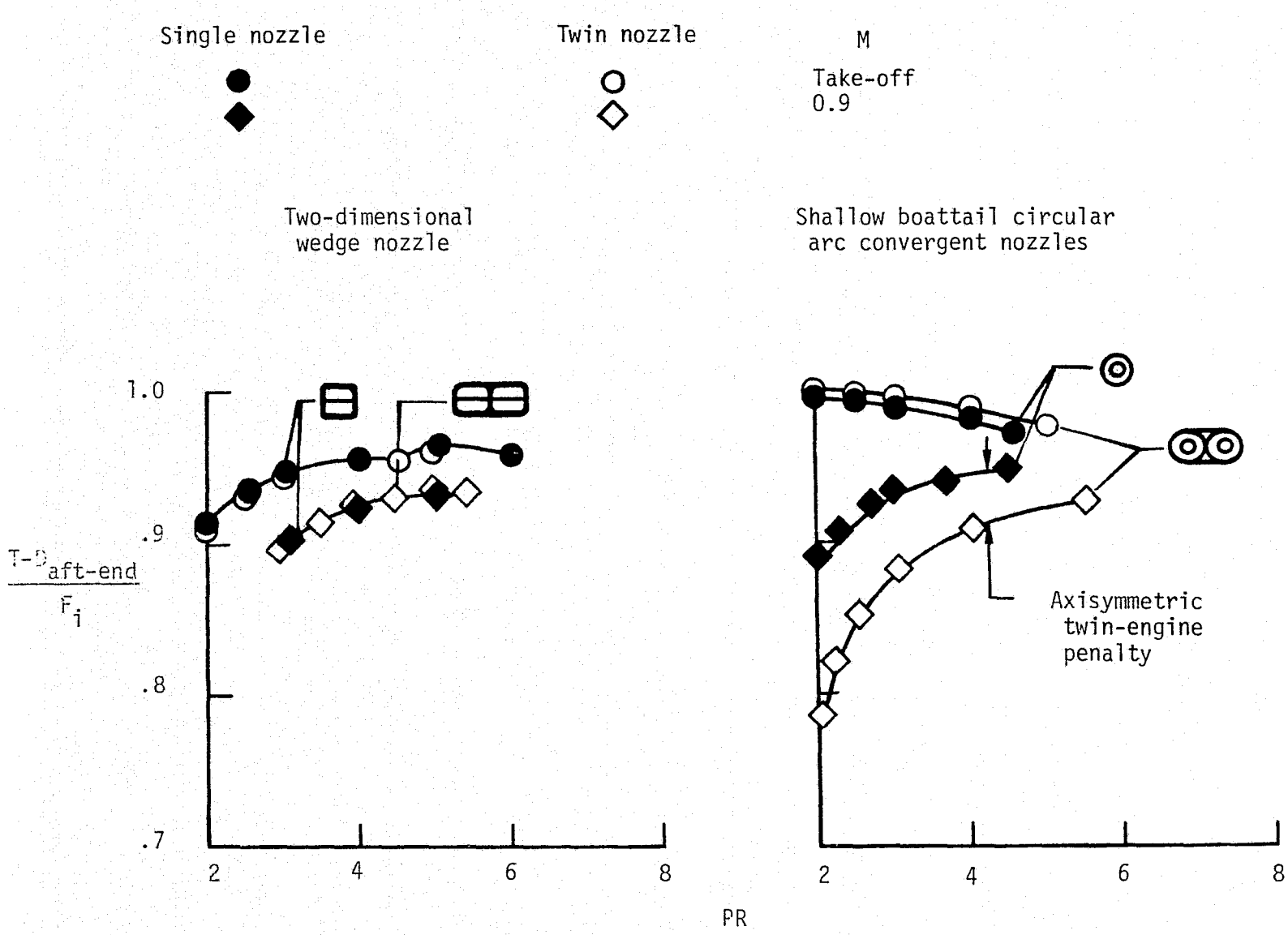

Figure 19.- Comparison of twin-engine penalties for axisymmetric and 2-D wedge nozzle installations. Dry power nozzle.

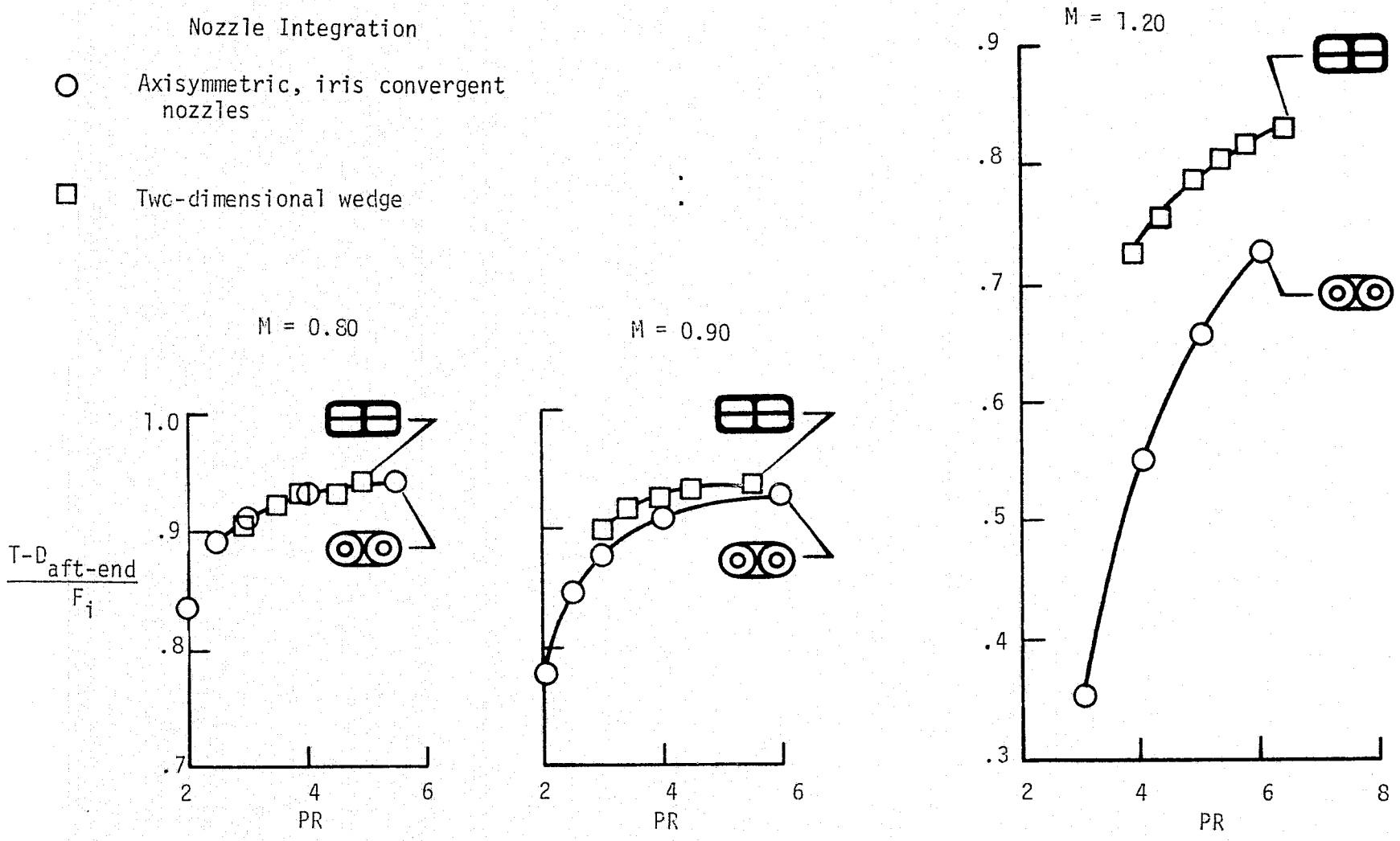

Figure 20.- Comparison of twin axisymmetric and twin 2-D wedge dry power nozzle performance.

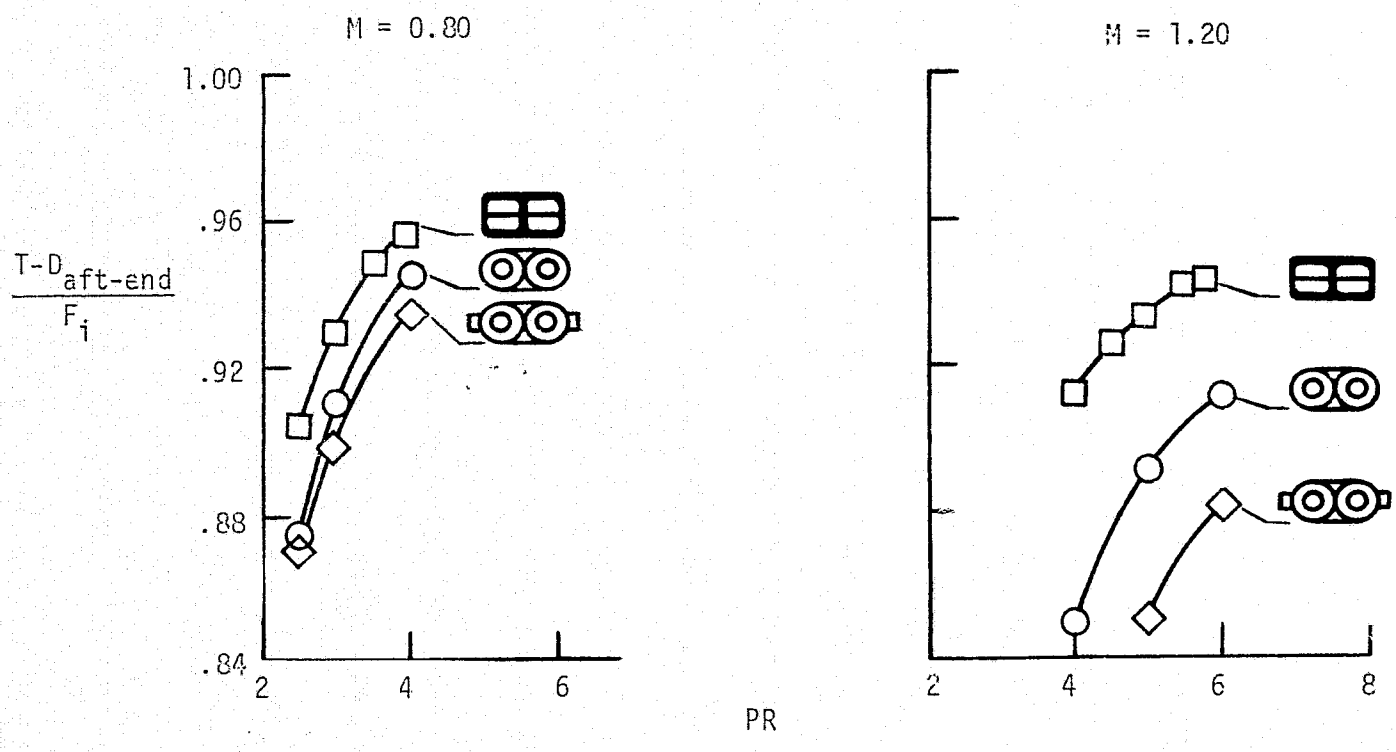

Figure 21.- Comparison of twin axisymmetric and twin 2-D wedge max A/B power performance.

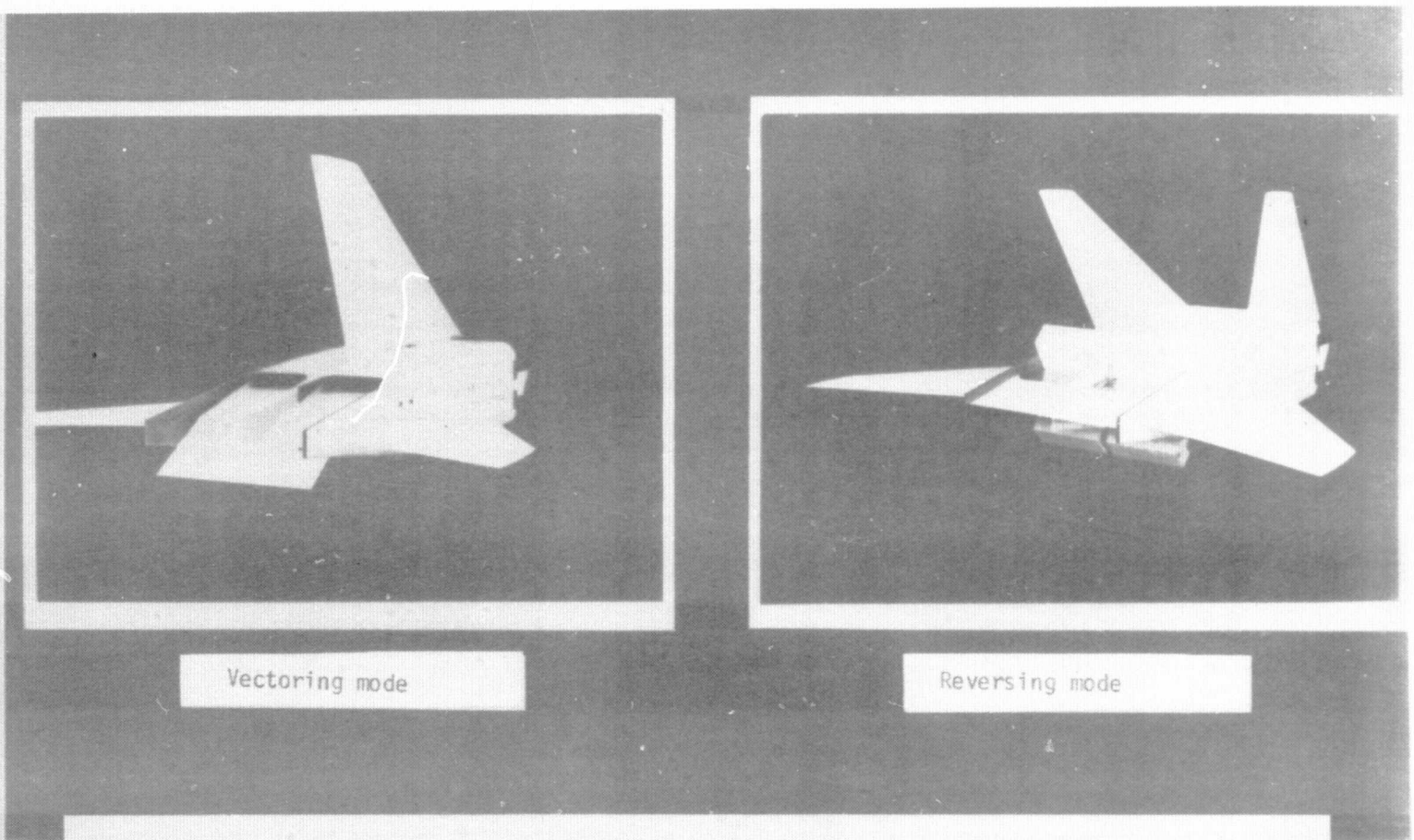

Figure 22.- Photographs of thrust vectoring and reversing nozzle configurations.

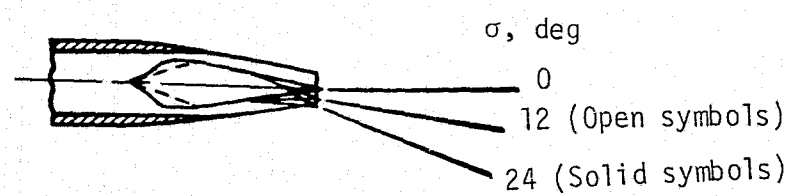

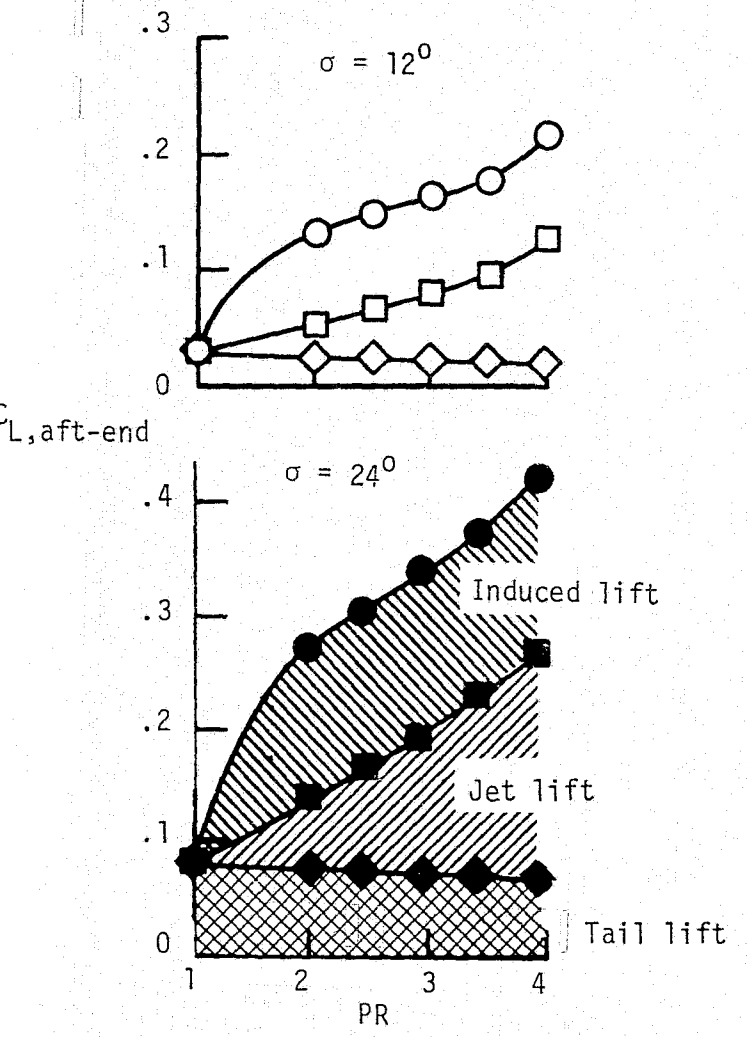

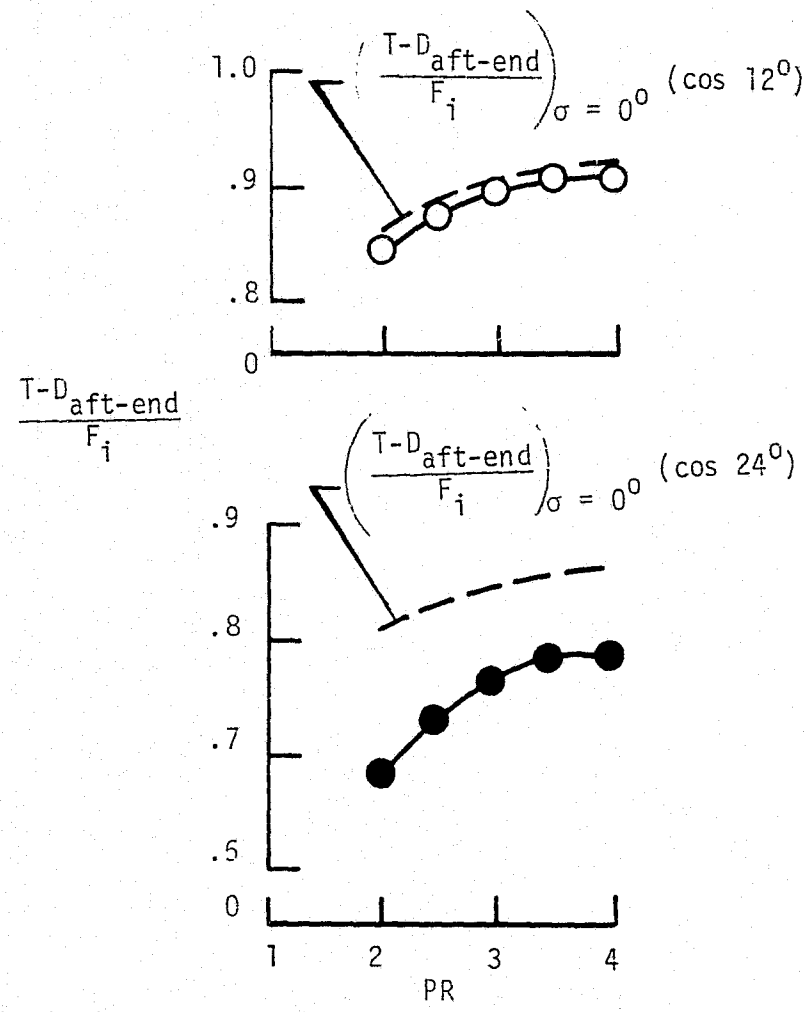

Figure 23.- Thrust vectoring characteristics of cambered wedge.

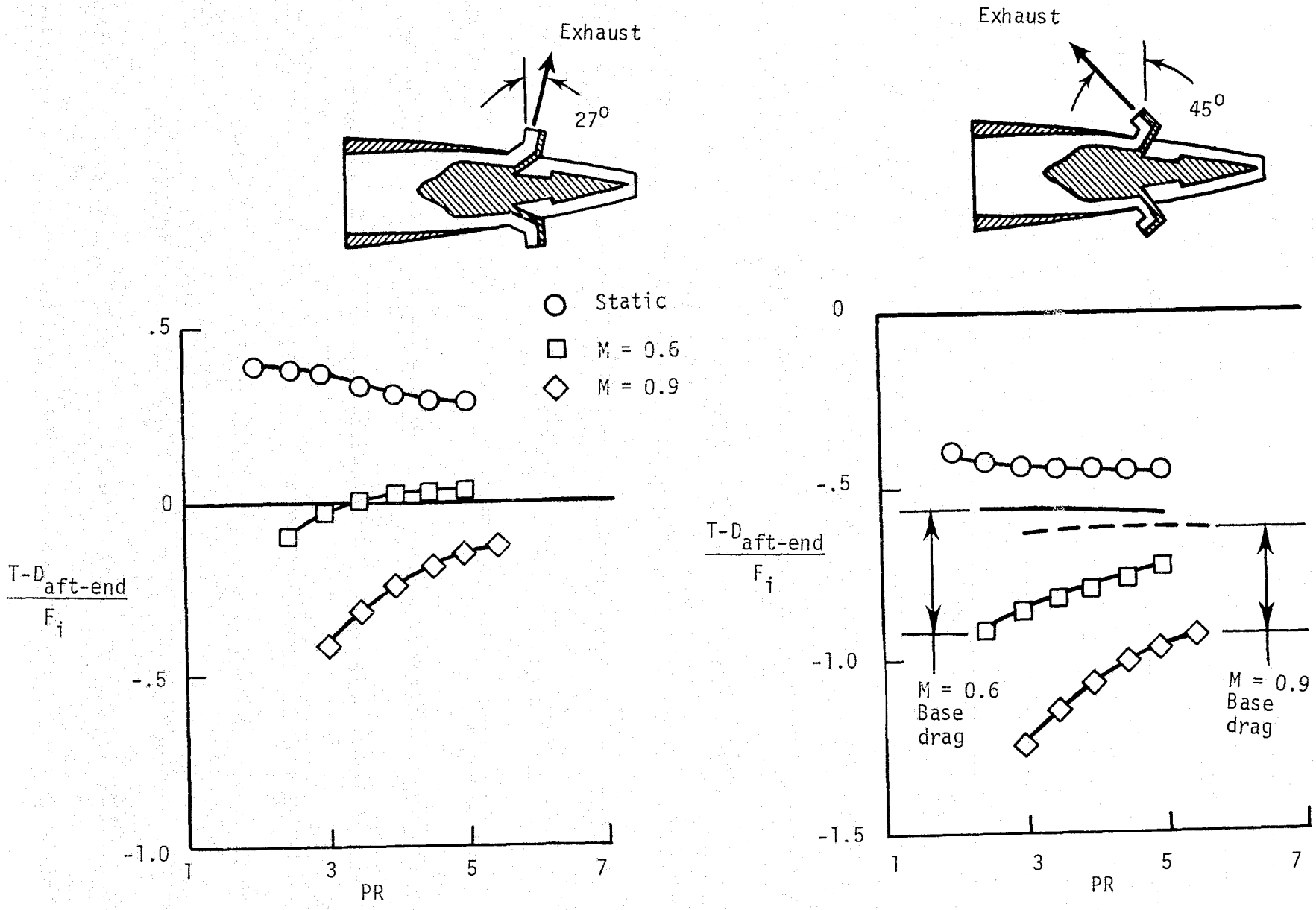

Figure 24.- Thrust reversing characteristics at deployments of 50 percent and 100 percent.

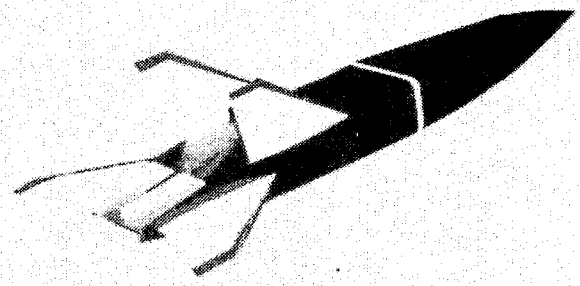

Aero-Propulsion Performance
- Small penalty at take-off/low speed
- High cruise performance above M = 0.8
- Significantly high dry-power performance at M = 1.20
- High afterburner-power performance
- Low pressure drag from empennage interference

Thrust Vectoring
- Significant body-alone gain factor achieved
- 12^{0} Vector more efficient for horizontal tail induced lift
- 24^{0} Vector wedge drag significant at M = 0.9

Thrust Reversing
- Static 45 percent reverse thrust
- In-flight reverse thrust over 100 percent
- Rudder effectiveness reduced 50 percent
- Operation appears smooth

Figure 25.- Summary of twin-engine results.